Acta Math., 214 (2015), 1–60
DOI: 10.1007/s11511-015-0122-0

Constructing entire functions by quasiconformal folding

by

Christopher J. Bishop

Stony Brook University
Stony Brook, NY, U.S.A.

1. Introduction

One aspect of Grothendieck's theory of *dessins d'enfants* is that each finite plane tree T is associated with a polynomial p with only two critical values, ± 1, so that $T_p = p^{-1}([-1,1])$ is a plane tree equivalent to T (see e.g. [43], [34] and [35]). T_p is called the "true form" of T and we will refer to a tree that arises in this way as a "true tree". Polynomials with exactly two critical values are called Shabat polynomials or generalized Chebyshev polynomials.

To be more precise, a plane tree is a tree with a cyclic ordering of the edges adjacent to each vertex. Any embedding of a tree in the plane defines such orderings and conversely, given any such orderings there is a corresponding planar embedding. Any two embeddings corresponding to the same orderings can be mapped to each other by a homeomorphism of the whole plane. Whenever we refer to two plane trees being equivalent, this is what we mean (it implies, but is stronger than saying, that they are the same abstract tree).

The result cited above says that every plane tree is equivalent to some true tree, i.e., choosing the "combinatorics" (the tree and the edge orderings) determines a "shape" (the planar embedding up to conformal linear maps). In [10], it is shown that all shapes can occur, i.e., true trees are dense in all continua with respect to the Hausdorff metric. In this paper, we extend these ideas from finite trees and polynomials to infinite trees and entire functions. The role of the Shabat polynomials is now played by the Speiser class $\mathcal{S}$; these are transcendental entire functions f with a finite singular set $S(f)$ (the closure of the critical values and finite asymptotic values of f). Let $\mathcal{S}_n \subset \mathcal{S}$ be the functions with at most n singular values and $\mathcal{S}_{p,q} \subset \mathcal{S}$ be the functions with p critical values and q finite

The author was partially supported by NSF Grant DMS 13-05233.

asymptotic values. We will be particularly interested in $\mathcal{S}_{2,0}$, as these are the direct generalizations of the Shabat polynomials. Some of our applications will deal with the larger Eremenko–Lyubich class $\mathcal{B}$ of transcendental entire functions with bounded (but possibly infinite) singular sets.

Given an infinite planar tree T satisfying certain mild geometric conditions, we will construct an entire function in $\mathcal{S}_{2,0}$ with critical values exactly ± 1, so that $T_f = f^{-1}([-1,1])$ approximates T in a precise way (T_f is the quasiconformal image of a tree T' obtained by adding branches to T; there may be many extra edges, but they all lie in a small neighborhood of T). We then apply the method to solve a number of open problems, e.g., the area conjecture of Eremenko and Lyubich and the existence of a wandering domain for an entire function with bounded singular set.

What does an entire function in $\mathcal{S}_{2,0}$ "look like"? Suppose the critical values are ± 1 and let $T = f^{-1}([-1,1])$. Then T is an infinite tree whose vertices are the preimages of $\{-1,1\}$ and the connected components of $\Omega = \mathbb{C}\setminus T$ are unbounded simply connected domains. We can choose a conformal map τ from each component to the right half-plane $\mathbb{H}_r = \{x+iy : x>0\}$ so that $f(z) = \cosh(\tau(z))$ on Ω. See Figure 1. Our goal is to reverse this process, constructing f from T. If we start with a tree T, we can define conformal maps τ from the complementary components of T to $\mathbb{H}_r$ and then follow these by cosh. The composition $g(z) = \cosh(\tau(z))$ is holomorphic off T, but is unlikely to be continuous across T. We will give conditions on T that imply that we can modify g in a small neighborhood of T so that it becomes continuous across T and is quasiregular on the whole plane. Then the measurable Riemann mapping theorem gives a quasiconformal mapping ϕ on the plane so that $f = g\circ\phi$ is entire. The modification of g alters the combinatorics of T by adding extra branches, and the use of the mapping theorem moves the modified tree by the quasiconformal map ϕ, but the changes in both combinatorics and shape can be controlled. In many applications, the new edges and the dilatation of ϕ can be contained in a neighborhood of T that has area as small as we wish, while keeping the dilatation of ϕ uniformly bounded. In such cases, the tree for f can approximate T arbitrarily closely in the Hausdorff metric.

To fix notation, assume that T is an unbounded, locally finite tree such that every component Ω_j of $\Omega = \mathbb{C}\setminus T$ is simply connected. We also assume that $\Omega_j = \sigma_j(\mathbb{H}_r)$, where σ_j is a conformal map that extends continuously to the boundary and sends ∞ to ∞. The inverses of these maps define a map $\tau : \Omega \to \mathbb{H}_r$ that is conformal on each component (we let $\tau_j = \sigma_j^{-1}$ denote the restriction of τ to Ω_j). Whenever we refer to a conformal map $\tau : \Omega \to \mathbb{H}_r$, we always mean a map that arises in this way.

Since T is a tree, it is bipartite and we assume that the vertices have been labeled with ± 1 so that adjacent vertices always have different labels. If V is the vertex set of T,

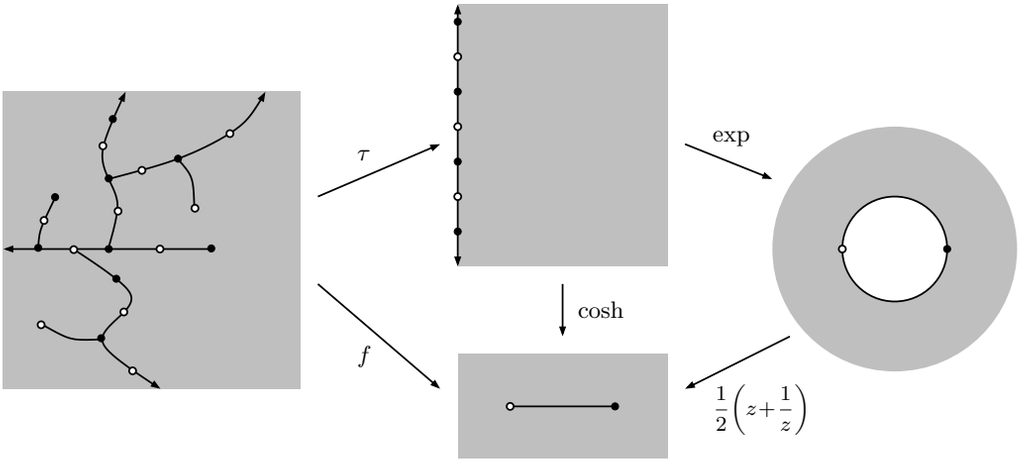

Figure 1. On $\Omega=\mathbb{C}\setminus T$ we can write $f=\cosh\circ\tau$, where τ is conformal on each component of Ω. The right side of the diagram is a geometric reminder of the formula $\cosh(z)=\frac{1}{2}(e^z+e^{-z})$ and shows that $\cosh\colon \mathbb{H}_r\to U=\mathbb{C}\setminus[-1,1]$ is a covering map.

let $V_j=\{z\in\partial\mathbb{H}_r\colon \sigma_j(z)\in V\}$; this is a closed set with no finite limit points. (It is tempting to write $V_j=\sigma_j^{-1}(V)$, but σ_j^{-1} is not defined on all of V and may be multi-valued where it is defined.) The collection $\mathcal{I}_j$ of connected components of $\partial\mathbb{H}_r\setminus V_j$ is called the *partition of* $\partial\mathbb{H}_r$ *induced by* Ω_j (different choices of the map τ_j only change the partition by a linear map). If $T=f^{-1}([-1,1])$ is the tree associated with an entire function with critical values ±1, then the associated partition is $\partial\mathbb{H}_r\setminus\pi i\mathbb{Z}$, and partition elements have equal size. In our theorem, "equal-size" partitions of $\partial\mathbb{H}_r$ are replaced by partitions such that (1) adjacent elements have comparable sizes and (2) there is a positive lower bound on the lengths of partition elements (both conditions holding for all complementary components of T with uniform bounds).

We will see below that the first condition is essentially local in nature and follows from "bounded-geometry" assumptions on T that are very easy to verify in practice. The second condition is more global; it depends on the shape of each complementary component near infinity and roughly says that the complementary components of T are "smaller than half-planes". For example if $\Omega=\{z\colon|\arg(z)|<\theta\}$ with unit spaced vertices on $T=\partial\Omega$, then the conformal map $\tau\colon\Omega\to\mathbb{H}_r$ is the power $z^{\pi/2\theta}$ and the lower bound condition is only satisfied if $\theta\leqslant\frac{1}{2}\pi$. We will see later that condition (2) can easily be restated in various ways using harmonic measure, extremal length or the hyperbolic metric in Ω, and is often easy to verify using standard estimates of these quantities.

For each $I\in\mathcal{I}$ let Q_I be the closed square in $\mathbb{H}_r$ that has I as one side, and let $V_{\mathcal{I}}$ be the interior of the union of all such squares. This is an open set in $\mathbb{H}_r$ that has $\partial\mathbb{H}_r$

in its closure (see Figures 2 and 6). For each $r>0$, define an open neighborhood of T by

$$T(r)=\bigcup_{e\in T}\{z:\operatorname{dist}(z,e)<r\operatorname{diam}(e)\},$$

where the union is over the edges of T. We shall show that there is fixed $r_0>0$ so that $V_{\mathcal{I}}\subset\tau_j(T(r_0)\cap\Omega_j)$; see Lemma 2.1.

Every (open) edge e of T corresponds via τ to exactly two intervals on $\partial\mathbb{H}_r$; we call these intervals the τ-images of e. Informally, we think of every edge e as having two sides, and each side has a single τ-image on $\partial\mathbb{H}_r$. The *τ-size* of e is the minimum length of the two τ-images. We say that T has *bounded geometry* if

(1) the edges of T are C^2 with uniform bounds;
(2) the angles between adjacent edges are bounded uniformly away from zero;
(3) adjacent edges have uniformly comparable lengths;
(4) for non-adjacent edges e and f, $\operatorname{diam}(e)/\operatorname{dist}(e,f)$ is uniformly bounded.

THEOREM 1.1. *Suppose that T has bounded geometry and every edge has τ-size $\geqslant\pi$. Then there is an entire f and a K-quasiconformal ϕ so that $f\circ\phi=\cosh\circ\tau$ off $T(r_0)$. K only depends on the bounded-geometry constants of T. The only critical values of f are ±1 and f has no finite asymptotic values.*

The idea of the proof of Theorem 1.1 is to replace the tree T by a tree T' so that $T\subset T'\subset T(r_0)$ and to replace τ by a map η that is quasiconformal from each component of $\Omega'=\mathbb{C}\setminus T'$ onto $\mathbb{H}_r$. We will prove that we can do this with a map η such that $\eta(V)\subset\pi i\mathbb{Z}$, $\eta=\tau$ off $T(r_0)$ and so that $g=\cosh\circ\eta$ is continuous across T'. The latter condition will imply that g is quasiregular on the whole plane and hence, by the measurable Riemann mapping theorem, there is a quasiconformal $\phi\colon\mathbb{C}\to\mathbb{C}$ such that $f=g\circ\phi^{-1}$ is entire. Since g is locally one-to-one except at the vertices of T, the only critical values are ±1. It is also easy to see that there are no finite asymptotic values and this proves the theorem. (In fact, any preimage of any compact set K of diameter $r<2$ will only have compact connected components. This condition rules out finite asymptotic values.)

The difficult part is constructing η so that $\cosh\circ\eta$ is continuous across T'. Note that η itself cannot be continuous across edges of T'; as z traverses an edge of T', the two τ-images of z under η will move along $\partial\mathbb{H}_r$ in different directions, so they can agree at most once on the edge. To make $\cosh\circ\eta$ continuous, we need cosh to identify the two images of z; this is the same as saying that the two images have equal distance from $2\pi i\mathbb{Z}$. We will build η so that

(1) η preserves normalized arclength measure on edges of T';
(2) η preserves vertex parity.

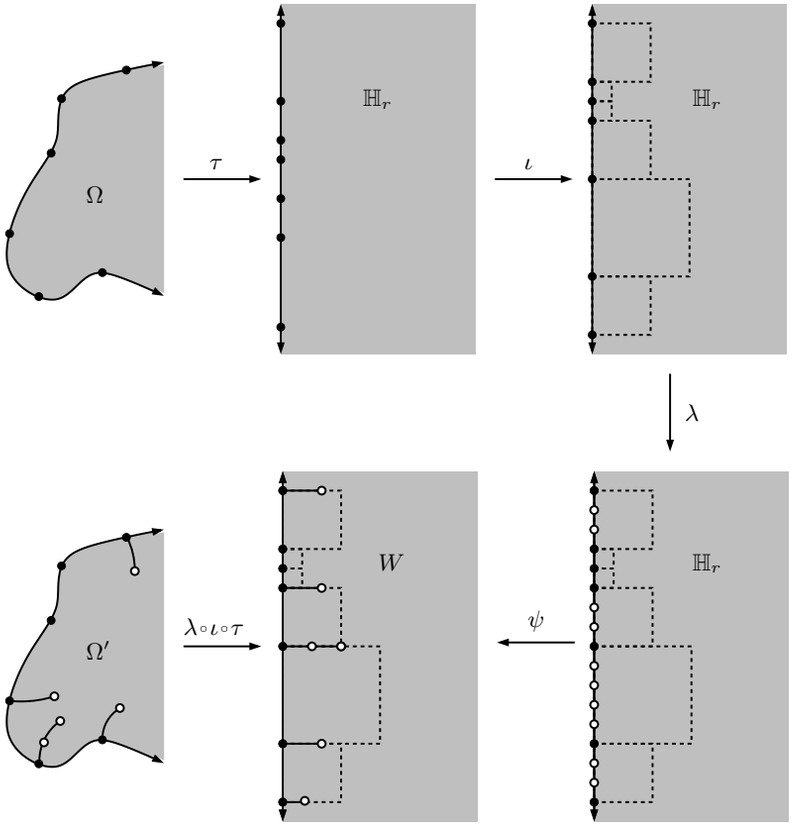

Figure 2. The map η is built as a composition: τ maps Ω to $\mathbb{H}_r$, ι sends vertices to integer points, λ makes the map preserve arclength and ψ "folds" the boundary. $V_{\mathcal{I}}$ is the union of the dashed squares.

By *normalized* arclength, we mean arclength scaled so that each edge has measure π. Condition (2) means that a vertex with label -1 is mapped to a point of $(2\pi i\mathbb{Z}+\pi i)\subset\partial\mathbb{H}_r$ and a vertex with label 1 is mapped to $2\pi i\mathbb{Z}$. Thus the value of $\cosh\circ\eta$ at a vertex is the same as the label of that vertex. This implies that $\cosh\circ\eta$ is well defined and continuous at the vertices of T; the first condition then implies that it is continuous across the edges.

Let η_j denote the restriction of η to the component Ω_j. We build η_j by post-composing τ_j with quasiconformal maps (see Figure 2):

$$\eta_j\colon \Omega_j \xrightarrow{\tau_j} \mathbb{H}_r \xrightarrow{\iota_j} \mathbb{H}_r \xrightarrow{\lambda_j} \mathbb{H}_r \xrightarrow{\psi_j} W_j \subset \mathbb{H}_r.$$

As noted earlier, the map τ_j sends vertices of T to a discrete set $V_j\subset\partial\mathbb{H}_r$ and $\mathcal{I}_j$ denotes the complementary components of V_j. By assumption, all these intervals have length $\geqslant\pi$. Let $\mathcal{Z}$ be the collection of the connected components of $\partial\mathbb{H}_r\setminus\pi i\mathbb{Z}$. We

will construct $\iota_j\colon \mathbb{H}_r \to \mathbb{H}_r$ to be a quasiconformal map that sends each point of V_j into $\pi i\mathbb{Z}$ and sends each interval of $\mathcal{I}_j$ to an interval of length $(2n+1)\pi$ (an odd multiple of π). Moreover, $\iota_j \circ \tau_j$ preserves vertex parity. These "odd-length" intervals give a new partition of $\partial\mathbb{H}_r$ that we call $\mathcal{K}_j$. The proof that ι_j exists is quite simple; see Lemma 3.2.

Next, we construct a quasiconformal map $\lambda_j\colon \mathbb{H}_r \to \mathbb{H}_r$ that fixes the endpoints of $\mathcal{K}_j$ and is such that $|(\lambda_j \circ \iota_j)'|/|\sigma_j'|$ is a.e. constant on each element of $\mathcal{K}_j$. Existence of λ_j follows from the bounded geometry of T (see Theorem 4.3). Informally, this property says that $\lambda_j \circ \iota_j \circ \tau_j$ multiplies length on each side of $\partial\Omega_j$ by a constant factor: if a side is mapped to an interval $K \in \mathcal{K}_j$ of length $(2n+1)\pi$, then normalized length on that side is multiplied by $2n+1$. Thus this side of T is mapped to a union of $2n+1$ elements of $\mathcal{Z}$, whereas we want it to map to a single element. The way to fix this is to add $2n$ extra sides to T, so that the original side and all of the new sides each map to elements of $\mathcal{Z}$. This is accomplished with the following lemma that describes the "quasiconformal folding" of the paper's title. The proof of Lemma 1.2 is the main technical contribution of this paper.

LEMMA 1.2. *Suppose that $\mathcal{K}$ is a partition of $\partial\mathbb{H}_r$ into intervals with endpoints in $\pi i\mathbb{Z}$ and lengths in $(2\mathbb{N}+1)\pi$ and suppose adjacent intervals have comparable lengths, with a uniform constant M. Then there is a quasiconformal map $\psi\colon \mathbb{H}_r \to W \subset \mathbb{H}_r$ so that*

(1) *ψ is the identity off $V_{\mathcal{K}}$;*
(2) *ψ is affine on each component of $\mathcal{Z} = \partial\mathbb{H}_r \setminus \pi i\mathbb{Z}$;*
(3) *each element $K \in \mathcal{K}$ contains an element of $\mathcal{Z}$ that is mapped to K by ψ;*
(4) *for any $x, y \in \mathbb{R}$, $\psi(ix) = \psi(iy)$ implies $\cosh(ix) = \cosh(iy)$.*

The image domain $W = \psi(\mathbb{H}_r)$ will be equal to $\mathbb{H}_r$ minus a countable union of finite trees (with linear edges) rooted at the endpoints of $\mathcal{K}$. The map ψ is constructed by triangulating both Ω and W in compatible ways (i.e., there is a one-to-one correspondence between the triangulations so that adjacency along edges is preserved). The linear maps between corresponding triangles then join together to define a piecewise linear map. Although each triangulation has infinitely many elements, all the triangles come from a finite family (up to Euclidean similarities) and thus the quasiconformal constant of all the linear maps is uniformly bounded. The proof of the lemma thus reduces to the construction of W and the two triangulations; it is essentially just a "proof-by-picture" (although it takes several intricate figures to describe all the details).

Figure 3 shows a simplified version of the main idea. We do the construction separately in each rectangle in $\mathbb{H}_r$ that has a "left-side" that is an element $K \in \mathcal{K}$ in $\partial\mathbb{H}_r$. Outside these rectangles, ψ is the identity. If K has length π then no folding is needed; we just take ψ to be the identity in such a rectangle. If K has length $(2n+1)\pi$, then K

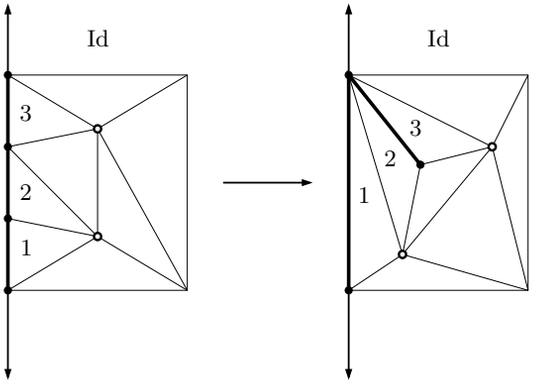

Figure 3. This shows a simple folding. Here an interval K of length 3π is folded into $\mathbb{H}_r$ so that one interval is expanded and the other two are sent to two sides of a slit. The map ψ is piecewise linear on the triangulations. Since there are only finitely many triangles, it is clearly quasiconformal. Simple foldings have a quasiconstant that grows with the size of K, but that can be performed independently for different K's. The general foldings used to prove Lemma 1.2 will have quasiconstant bounded independent of K, but they require careful coordination between adjacent intervals.

contains $2n+1$ elements of $\mathcal{Z}$; ψ expands one of these to K and the other $2n$ are affinely mapped to sides of a tree inside $\mathbb{H}_r$. One way of doing this is illustrated in Figure 3. On the left is a rectangle that has been triangulated with eight triangles. On the right is a slit rectangle that has been similarly triangulated. The reader can easily verify that the two triangulations are compatible and that the resulting piecewise linear map is the identity on the top, bottom and right sides of the rectangle, that it maps the boundary interval labeled "1" to all of K, and that it maps the intervals labeled "2" and "3" to opposite sides of the slit. Thus the intervals 2 and 3 are "folded" into a single interval.

This particular type of folding is called *simple folding*. It can be performed for each element $K \in \mathcal{K}$ independent of what we do for neighboring elements, because the folding map is the identity on the sides of the rectangle meeting neighboring rectangles. However, the quasiconstant of the folding map depends on the number of sides being folded; as the size of K increases to ∞, so does the quasiconstant of the folding map. For some applications, this is not important. For example, in [11], I use simple foldings to build functions in the Eremenko–Lyubich class $\mathcal{B}$. In that paper, the corresponding partition elements have lengths bounded both below and above, so simple folding gives a quasiconformal map. Thus [11] may be considered as a "gentle introduction" to the folding construction in this paper. In this paper, however, the partition elements do not have an upper bound (at least not in the most interesting applications) and we need the folding map to have quasiconstant bounded independent of the size of K. This is achieved by replacing the slit rectangle in Figure 3 by a rectangle with complicated

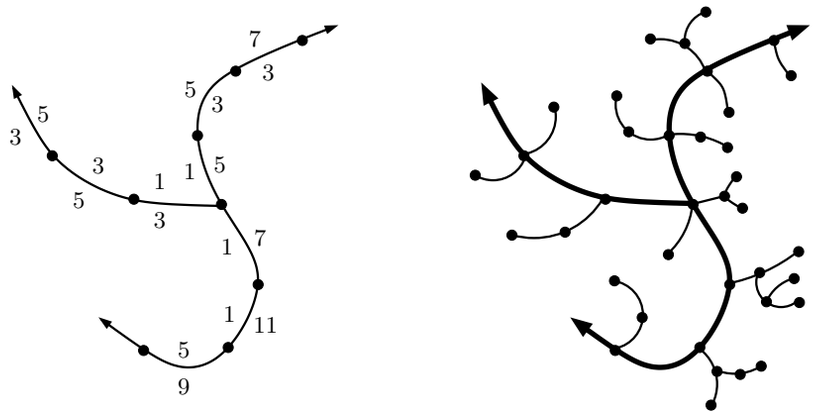

Figure 4. On the left is a tree T with possible τ-lengths of sides marked. On the right is the tree T' which is formed by adding a tree with n edges at one endpoint of a T-edge with label $2n+1$.

finite trees removed; moreover, the constructions for adjacent K's must now be carefully joined, which requires that the corresponding trees have approximately the same size; this is the source of the "adjacent intervals must have comparable lengths" condition in our theorem.

We now return to our description of the map η_j. Suppose ψ_j is the map given by Lemma 1.2 when applied to the partition $\mathcal{K}_j$ corresponding to the component Ω_j. Let

$$\Omega_j' = (\lambda_j \circ \iota_j \circ \tau_j)^{-1}(W) = (\psi_j \circ \lambda_j \circ \iota_j \circ \tau_j)^{-1}(\mathbb{H}_r) \subset \Omega_j.$$

This is just Ω_j with countably many finite trees removed, each rooted at a vertex of T. See Figure 4. The composition $\eta_j = \psi_j^{-1} \circ \lambda_j \circ \iota_j \circ \tau_j$ maps Ω_j to $\mathbb{H}_r$ and satisfies the following properties:

(1) η_j is uniformly quasiconformal from each component of Ω' to $\mathbb{H}_r$;
(2) η_j maps vertices of T to points in $\pi i\mathbb{Z}$ of the correct parity;
(3) η_j preserves normalized length on all sides of T'.

These conditions imply that $g = \cosh \circ \eta$ is continuous across T'. Every edge of T' is either an edge of T, in which case it is rectifiable, or it is a quasiconformal image of a line segment. Thus T' is removable for quasiregular maps and hence g is quasiregular on the whole plane, as desired. Finally, ι_j, λ_j and ψ_j are all the identity off $V_{\mathcal{I}}$. By Lemma 2.1, this implies that $\eta_j = \tau_j$ off $T(r_0)$ for some fixed r_0, and this completes the proof of Theorem 1.1 (except for proving the various results described above).

Theorem 1.1 is simple to apply and suffices to create many interesting examples, but it can be generalized in several useful ways:

High-degree critical points and asymptotic values. The bounded geometry of T places an upper bound on the degree of the critical points of f. In §7 we will state an

alternative version that allows us to build functions with arbitrarily-high-degree critical points. The tree T will be replaced by a more general graph and the map τ will map the bounded complementary components to disks. Several examples in this paper use high-degree critical points, so we will need this more general version of Theorem 1.1. A similar modification allows us to introduce finite asymptotic values.

Alternative domains. In this paper, we mainly use Theorem 1.1 to construct entire functions, but the proof applies to any unbounded tree T on a Riemann surface S that partitions the surface into simply connected domains. Some examples will be given in §§14–16. For the method to work, we need a conformal map τ of the components of $S\setminus T$ to $\mathbb{H}_r$ so that vertices of T induce partitions on $\mathbb{H}_r$ with the properties that (1) adjacent intervals have comparable sizes and (2) interval lengths are $\geqslant\pi$. The construction then gives a quasiregular $g=\cosh\circ\eta$ on S. The measurable Riemann mapping theorem says that we can find a quasiconformal $\phi\colon S\to S'$ so that $f=g\circ\phi^{-1}$ is holomorphic. When $S=\mathbb{C}$ we can take $S'=S=\mathbb{C}$ since there is no alternative conformal structure on $\mathbb{C}$. Similarly if $S=\mathbb{D}$ or S is a once or twice punctured plane. In general, S and S' are homeomorphic, but need not be conformally equivalent.

Weakening τ-size $\geqslant\pi$. If $\tau\colon\Omega\to\mathbb{H}_r$ is conformal, then so is any map obtained by multiplying τ by a positive constant on each component (possibly different constants on different components). Thus Theorem 1.1 will apply to some τ if we know that each component Ω_j has a conformal map to $\mathbb{H}_r$ that induces a partition of $\partial\mathbb{H}_r$ with some positive lower bound on the interval lengths (having a positive lower bound is independent of which conformal map we choose). In most of our examples, we simply have to verify a positive lower bound for each component separately and then multiply by constants to get a τ that works in Theorem 1.1. One important consequence is that if there is a choice of τ that gives a neighborhood $T(r)$ of finite area, then by multiplying τ by a positive factor and adding extra vertices, we can arrange for $T(r)$ to have an area as small as we wish. Adding the extra vertices does not effect the bounded-geometry constant, so the quasiconformal correction map ϕ will have uniformly bounded QC-constant as we rescale τ and add vertices, but the support of its dilatation has area tending to zero, and hence ϕ tends to the identity as we rescale. Therefore if a tree T satisfies the conditions of Theorem 1.1 and $T(r)$ has finite area, then T is a limit of trees corresponding to entire functions with exactly two singular values (critical values at ±1).

§§2–6 complete the details in the proof of Theorem 1.1 outlined above. §7 states the generalization that allows high-degree critical points and asymptotic values. §8 describes methods for verifying the τ-length condition in Theorem 1.1. The remaining sections describe various examples that can be constructed with these methods. We are mostly

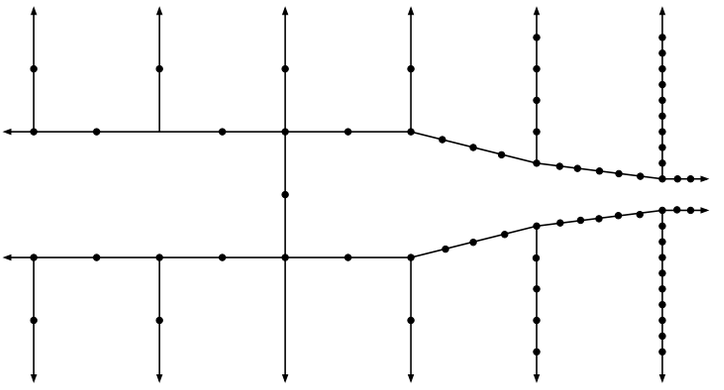

Figure 5. A tree corresponding to a function in $\mathcal{S}$ that grows as quickly as we wish. One must verify that the tree has bounded geometry (easy) and choose τ in each component so that every edge has τ-size $\geqslant\pi$ (also easy).

interested in functions in the Speiser class $\mathcal{S}$ (finite singular sets) and Eremenko–Lyubich class $\mathcal{B}$ (bounded singular set). Among our applications will be

- counterexamples to the area conjecture in $\mathcal{S}$;
- counterexample to the strong Eremenko conjecture in $\mathcal{S}$;
- spiraling tracts with arbitrary speed in $\mathcal{S}$;
- building finite-type maps (after Epstein) into compact surfaces;
- a counterexample to Wiman's minimum modulus conjecture in $\mathcal{S}$;
- a wandering domain for $\mathcal{B}$.

Entire functions with wandering domains have been constructed before (the first by Baker in [3]), but not in $\mathcal{B}$. Functions in $\mathcal{S}$ cannot have wandering domains (Eremenko and Lyubich in [22], and Goldberg and Keen in [28]), so our example shows the sharpness of this result. In our example, there are no finite asymptotic values and only countably many critical values, and these accumulate at only two points.

As a first simple example of how Theorem 1.1 can be applied, consider the tree drawn in Figure 5. All the components are essentially half-strips, except for one, Ω_+, that contains the positive real axis and which narrows as quickly as we wish. It is easy to place vertices so that T has bounded geometry, the τ-size of every edge is $\geqslant\pi$ (see §8 for details) and so that $T(r_0)$ misses $[1,\infty)$. Thus Theorem 1.1 says there is a quasiregular g that agrees with $\cosh\circ\tau$ on $[1,\infty)$, where $\tau\colon\Omega_+\to\mathbb{H}_r$ is conformal. By narrowing Ω_+ we can make τ grow as quickly as we wish. Since ϕ is uniformly quasiconformal, it is bi-Hölder with a fixed constant, and so $f=g\circ\phi^{-1}\in\mathcal{S}_{2,0}$ also grows as quickly as we wish. Such examples are originally due to Merenkov [37] by a different method.

The use of quasiconformal techniques to build and understand entire functions with finite singular sets has a long history with its roots in the work of Grötzsch, Speiser,

Teichmüller, Ahlfors, Nevanlinna, Lavrentiev and many others. The earlier work was often phrased in terms of the type problem for Riemann surfaces: deciding if a simply connected surface built by branching over a finite singular set was conformally equivalent to the plane or to the disk (in the first case the uniformizing map gives a Speiser class function). Such constructions play an important role in value distribution theory; see [16] for an excellent survey by Drasin, Gol′dberg and Poggi-Corradini of these methods and a very useful guide to this literature. Also see Chapter VII of [27] by Gol′dberg and Ostrovskii which is the standard text in this area (updated in 2008 with an appendix by Eremenko and Langley on more recent developments).

Much recent work on quasiconformal mappings is motivated by applications to holomorphic dynamics, such as quasiconformal surgery, a powerful method that has been used in rational dynamics to construct new examples with desired properties, estimate the number of attracting cycles, and (perhaps most famously) prove the non-existence of wandering domains. See the recent book [14] by Branner and Fagella for a discussion of these, and other, highlights of this literature. In the iteration theory of entire functions, the Speiser class provides an interesting mix of structure (like polynomials, the quasiconformal equivalence classes are finite-dimensional [22]) and flexibility (as indicated by the current paper). Examples of entire functions with exotic dynamical properties have also been constructed using infinite products (e.g., [1], [3], [6], [9]) approximation results such as Arakelian's and Runge's theorems (e.g., [21]) or Cauchy integrals (e.g., [44], [45], [39]). Generally speaking, these methods do not give such precise control of the singular set as quasiconformal constructions do.

A version of Theorem 1.1 for the Eremenko–Lyubich class $\mathcal{B}$ is given in [11]. Instead of taking the complement of an infinite tree, that paper takes a locally finite union Ω of disjoint, simply connected domains $\{\Omega_j\}_j$ and a choice of conformal map $\tau_j\colon\Omega_j\to\mathbb{H}_r$ on each component, defining a holomorphic map $\tau\colon\Omega\to\mathbb{H}_r$. The result states that for any $\varrho>0$, the restriction of e^τ to $\Omega(\varrho)=\tau^{-1}(\mathbb{H}_r+\varrho)$ has a quasiregular extension to the plane (with quasiconstant depending only on ϱ) and the extension is bounded off $\Omega(\varrho)$. Thus there is $f\in\mathcal{B}$ and a quasiconformal ϕ so that $f\circ\phi=e^\tau$ on $\Omega(\varrho)$. The proof in [11] is analogous to, but easier than, the construction in this paper. In [12] it is shown that we can even take $f\in\mathcal{S}$, but not always with the "bounded off $\Omega(\varrho)$" conclusion. Making the geometric distinctions between $\mathcal{B}$ and $\mathcal{S}$ precise is the main purpose of [12].

Acknowledgements. This paper had its start during a March 2011 conversation between myself and Alex Eremenko about the behavior of polynomials with exactly two critical values. His questions led to the paper [10] on dessins and Shabat polynomials, and the current paper adapts those ideas to transcendental entire functions. I thank Alex Eremenko and Lasse Rempe-Gillen for their lucid descriptions of the problems, their al-

most instantaneous responses to my emails, and for their generous sharing of history, open problems and ideas. Also thanks to Simon Albrecht; he carefully read an earlier draft and made numerous helpful suggestions that fixed some errors and improved the exposition. Similarly, Xavier Jarque read the manuscript and provided many comments; his questions prompted a variety of improvements and corrections to the text. Two anonymous referees provided thoughtful suggestions that improved the paper's clarity and correctness and they provided further references to related literature. I thank them for their careful reading of the manuscript and for their hard work to make it easier for others to read.

2. A neighborhood of the tree

LEMMA 2.1. *$\tau^{-1}(V_{\mathcal{I}})\subset T(r_0)$ for some $r_0\leqslant 25.3$.*

Proof. For an interval $I\subset\partial\mathbb{H}_r$, let

$$W(I,\alpha)=\{z\in\mathbb{H}_r:\omega(z,I,\mathbb{H}_r)>\alpha\},$$

where ω denotes harmonic measure. The set in $\mathbb{H}_r$ where I has harmonic measure bigger than α is the same as the set where I subtends angle $\geqslant\pi\alpha$; this is a crescent bounded by I and the arc of the circle in $\mathbb{H}_r$ that makes angle $\pi(1-\alpha)$ with I. See Figure 6. Some simple geometry shows that $W\big(I,\frac{1}{2}\big)\subset Q_I\subset W\big(I,\frac{1}{4}\big)$ and hence $V_{\mathcal{I}}\subset\bigcup_{I\in\mathcal{I}}W\big(I,\frac{1}{4}\big)$ (recall that Q_I is the square in $\mathbb{H}_r$ with I as one side). Thus $\tau^{-1}(V_{\mathcal{I}})$ is contained in the set of points z in Ω such that some single edge e of T has harmonic measure $\omega(z,e,\Omega)\geqslant\frac{1}{4}$. Beurling's projection theorem (see [24, Corollary III.9.3]) then implies

$$\frac{1}{4}\leqslant\omega(z,e,\Omega)\leqslant\frac{4}{\pi}\arctan\sqrt{\frac{\operatorname{diam}(e)}{\operatorname{dist}(z,e)}}.$$

Hence

$$\operatorname{dist}(z,e)\leqslant\arctan^2\big(\tfrac{1}{16}\pi\big)\operatorname{diam}(e),$$

and so $\tau^{-1}(V_{\mathcal{I}})\subset T(r_0)$, where $r_0=\arctan^2\big(\frac{1}{16}\pi\big)\approx 25.27$. □

3. Integerizing a partition

As noted in the introduction, one of the "easy" steps of the proof is to approximate a partition of a line by another partition that has integer endpoints and odd lengths. We start with a simple lemma.

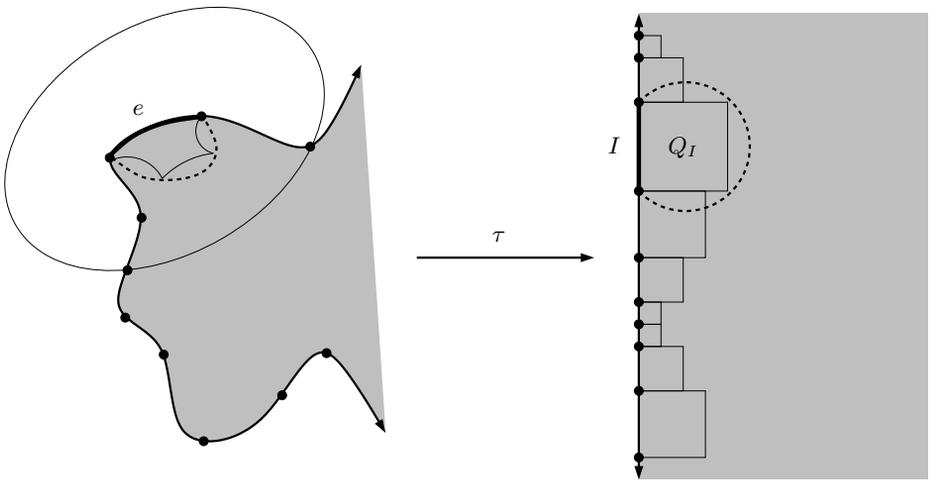

Figure 6. The set $V_{\mathcal{I}}$ is a union of squares Q_I in $\mathbb{H}_r$, each with one side that is an element $I \in \mathcal{I}$. The square Q_I is contained in the crescent region where I has harmonic measure $\geqslant \frac{1}{4}$. If I corresponds via τ to an edge e of the tree T, then Q_I must map to a region contained in $\{z : \operatorname{dist}(z,e) \leqslant r_0 \operatorname{diam}(e)\}$, where r_0 is the constant computed in Lemma 2.1.

LEMMA 3.1. *Suppose that $\mathcal{I}=\{I_j\}_j$ is a bounded-geometry partition of the real numbers (i.e., adjacent intervals have comparable lengths) so that every interval has length $\geqslant 1$. Then there is second partition $\mathcal{J}=\{J_j\}_j$ such that*

- *every endpoint of $\mathcal{J}$ is an integer*;
- *the length of J_j is an odd integer*;
- *I_j and J_j have lengths differing by $\leqslant 2$*;
- *the left endpoints of I_j and J_j are within distance $\frac{5}{2}$ of each other*; *similarly for the right endpoints.*

Proof. After translating by at most $\frac{1}{2}$, we may assume that I_0 contains a non-trivial interval with integer endpoints and odd length. Let J_0 be the maximal such interval in I_0. For $j>0$, let the left endpoint of J_j be the right endpoint of J_{j-1}. Choose its right endpoint to be the largest integer that is less than or equal to the right endpoint of I_j and so that J_j has odd length. Since I_j has length $\geqslant 1$, there is such a choice. Then conditions (1)–(3) all hold and (4) holds with constant 2. A similar argument holds for $j<0$. When we undo the initial translation, (1)–(3) all hold with the same constants and (4) holds with $\frac{5}{2}$. □

LEMMA 3.2. *There is a quasiconformal map ι of the upper half-plane $\mathbb{H}_u=\{x+iy : y>0\}$ to itself that sends the partition $\mathcal{I}$ in Lemma 3.1 to the partition $\mathcal{J}$. The map ι is the identity on $\mathbb{H}_u+i=\{x+iy : y>1\}$ and the dilatation is bounded independently of $\mathcal{I}$.*

Proof. We now define a map $\psi_1 : \mathbb{R} \to \mathbb{R}$ as the piecewise linear map that sends I_j

to J_j. This is clearly bi-Lipschitz. This boundary mapping ψ_1 can be extended to a quasiconformal mapping of $\mathbb{H}_u$ that is the identity off the strip $S=\{x+iy:0<y<1\}$ by linearly interpolating the identity on $\{x+iy:y=1\}$ with ψ_1 on $\mathbb{R}$. It is easy to see that this defines a bi-Lipschitz (and hence quasiconformal) map of S to itself, that extends to the identity on the rest of $\mathbb{H}_u$. □

4. Length-respecting maps

We start by verifying some claims made in the introduction. Let Ω_j be a component of $\Omega=\mathbb{C}\setminus T$ and let $\mathcal{I}_j$ be the partition of $\partial\mathbb{H}_r$ induced by τ on the component Ω_j. Also recall that $V_{\mathcal{I}}\subset\mathbb{H}_r$ is the union of squares with sides in $\mathcal{I}_j$.

LEMMA 4.1. *If T is a bounded-geometry tree then adjacent elements of $\mathcal{I}_j$ have comparable lengths.*

Proof. Adjacent intervals $I, J\subset\partial\mathbb{H}_r$ corresponding to sides of adjacent edges e and f of T will have comparable lengths if and only if there is a point $z\in\mathbb{H}_r$ from which the harmonic measures of I and J, and both components of $\partial\mathbb{H}_r\setminus(I\cup J)$ are all comparable. But if we take a point $w\in\Omega$ with

$$\operatorname{dist}(w,e)\simeq\operatorname{dist}(w,f)\simeq\operatorname{dist}(w,\partial\Omega),$$

the bounded-geometry assumption and the conformal invariance of harmonic measure imply that this is true for $z=\tau(w)$. □

We say that a homeomorphism h of one rectifiable curve γ_1 to another rectifiable curve γ_2 *respects length* if it is absolutely continuous with respect to arclength and $|h'|$ is a.e. constant, i.e., $\ell(\tau(E))=\ell(E)\ell(\gamma_2)/\ell(\gamma_1)$, for every measurable $E\subset\gamma_1$. This generalizes the idea of a linear map between line segments.

LEMMA 4.2. *Suppose that $\eta:\Omega\to\mathbb{H}_r$ is quasiconformal on each of its connected components, maps the vertices of T into $\pi i\mathbb{Z}$ and is length respecting on each side of T. Also suppose that for each edge e in T, the two sides of e have equal τ-length. If $\cosh\circ\eta$ is continuous at all vertices of T, then it is continuous across all edges of T.*

Proof. Suppose that v and w are the endpoints of e, and $z\in e$. By assumption the two possible images of e under η have the same length and have their endpoints in $\pi i\mathbb{Z}$. Since $\cosh\circ\eta$ is continuous at w, both of its images have the same parity. Similarly for v. Therefore the length-respecting property implies that both images of z have the same distance from $2\pi i\mathbb{Z}$, which implies the result. □

THEOREM 4.3. *Let T be a bounded-geometry tree, Ω_j be a component of $\Omega=\mathbb{C}\setminus T$ and $\sigma_j\colon\mathbb{H}_r\to\Omega_j$ be the inverse to τ for this component. Suppose that the partition of $\partial\mathbb{H}_r$ induced by Ω_j has bounded geometry. Then there is a quasiconformal map $\beta\colon\mathbb{H}_r\to\mathbb{H}_r$ so that $\sigma_j\circ\beta$ is length-respecting on every element of $\mathcal{I}_j$. The map β is the identity on $V_j\subset\partial\mathbb{H}_r$ and on $\mathbb{H}_r\setminus V_{\mathcal{I}}$.*

Proof. Consider adjacent intervals $I,J\in\mathcal{I}_j$ corresponding to edges e and f of T with a common vertex v. The bounded-geometry condition states that e and f have comparable lengths and Lemma 4.1 says that I and J have comparable lengths.

Let θ be the interior angle of Ω formed by the edges e and f and let $\alpha=\theta/\pi$. Then

$$\left|\frac{d}{dx}\sigma_j(x)\right|\simeq\frac{\ell(e)}{\ell(I)}(x-a)^{\alpha-1},$$

on both I and J near the endpoint a.

Let K be the interval centered at a with length $\ell(K)=\frac{1}{4}\min\{\ell(I),\ell(J)\}$. Normalize so that $a=0$ and $\ell(K)=1$ and consider the map

$$\varphi(z)=\begin{cases} z|z|^{\alpha-1} & \text{for } |z|\leqslant 1,\\ z & \text{for } |z|>1.\end{cases}$$

Then $\varphi\circ\tau$ has a derivative that is bounded and bounded away from zero on $\sigma_j(K)$. The map φ is the identity outside the disk with diameter $\ell(K)$, and so is certainly the identity outside $V_{\mathcal{I}}$.

Now build a version of φ for every pair of adjacent edges to get a quasiconformal map $\varphi\colon\mathbb{H}_r\to\mathbb{H}_r$ that fixes every endpoint of our partition $\mathcal{I}$ and is the identity outside $V_{\mathcal{I}}$. For any interval $I\in\mathcal{I}$, we can use integration to define a bi-Lipschitz map $\varkappa\colon I\to I$ fixing each endpoint of I and so that the derivative of $\varkappa\circ\varphi\circ\tau$ has constant absolute value. By simple linear interpolation this $\varkappa$ can be extended to a bi-Lipschitz map of Q_I (the square in $\mathbb{H}_r$ with I as one side) that is the identity on the other three sides of Q_I. Doing this for every interval in the partition defines a quasiconformal $\varkappa$ on $\mathbb{H}_r$ that is the identity off $V_{\mathcal{I}}$. Clearly $\beta=\varkappa\circ\varphi$ satisfies the conclusions of Theorem 4.3, completing the proof. □

5. The folding map: building the tree

The following lemma is the central fact needed in the proof of Theorem 1.1. It was stated in the introduction, but to simplify notation we have rotated by 90 degrees and dilated by a factor of π. If $\mathcal{J}$ is a partition of $\mathbb{R}$ into intervals, we let $V_{\mathcal{J}}$ be the union of the squares in $\mathbb{H}_u=\{x+iy\colon y>0\}$ with bases in $\mathcal{J}$.

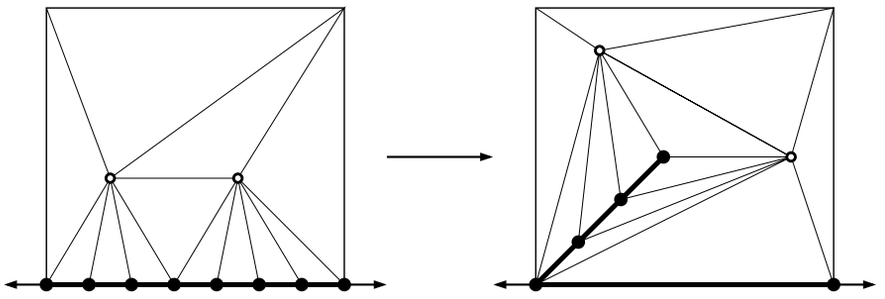

Figure 7. This simple tree is just a slit in the upper half-plane partitioned into n edges. The triangulations show how $\mathbb{H}_u$ can be mapped to the complement of the slit by a piecewise linear map that is the identity outside the indicated square.

LEMMA 5.1. *Let $\mathcal{J}=\{J_j\}_j$ be a partition of $\mathbb{R}$ into intervals with endpoints in $\mathbb{Z}$ and all odd lengths. Assume that any two adjacent elements have lengths within a factor of $M<\infty$ of each other. Then there is a map ψ of $\mathbb{H}_u=\{x+iy:y>0\}$ into itself and intervals $J_j'\subset J_j$, so that the following all hold*:

(1) *each J_j' has integer endpoints and length* 1;
(2) *ψ is the identity off $V_{\mathcal{J}}$*;
(3) *ψ is quasiconformal with a constant depending only on M*;
(4) *ψ is affine on each component of $\mathbb{R}\setminus\mathbb{Z}$*;
(5) *$\psi(J_j')=J_j$ for all j*;
(6) *$\psi(x)=\psi(y)$ implies that $x,y\in\mathbb{R}$ have the same distance to $2\mathbb{Z}$.*

The domain $\psi(\mathbb{H}_u)\subset\mathbb{H}_u$ will be constructed by removing finite trees, rooted at the endpoints of $\mathcal{J}$. It will be given as a certain quasiconformal image of a domain $W=\mathbb{H}_u\setminus\Gamma$, where Γ is a collection of finite trees rooted at points of $\mathbb{Z}$. In this section we describe Γ and W; in the next section we build the map ψ.

The simplest trees in the construction are just segments in $\mathbb{H}_u$ with a small number of vertices on them. We call these "0-level" trees or "simple foldings" and one such is illustrated in Figure 7. This is essentially the same as the folding illustrated in Figure 3 in the introduction. The triangulations induce a piecewise linear map that "folds" $\mathbb{H}_u$ into itself minus a slit. The map is the identity outside the indicated box.

Next we consider "j-level trees" for $j\geqslant 1$. We start with the trees $\widehat{T}_j$ illustrated in Figure 8. We normalize so that $\widehat{T}_j$ has convex hull $R_j=[0,2]\times[0,1-2^j]$. The edges of $\widehat{T}_j$ have an obvious partition into levels; there is one horizontal "base" edge at level 0 and 2^{j+1} edges at level j. We form the tree T_j by dividing each jth level edge of $\widehat{T}_j$ into 2^j edges, as shown in Figure 9. T_j and $\widehat{T}_j$ have the same topology, and although our proofs all refer to T_j, most of our figures will only show $\widehat{T}_j$ in place of T_j because the huge number of vertices in T_j are impractical to draw.

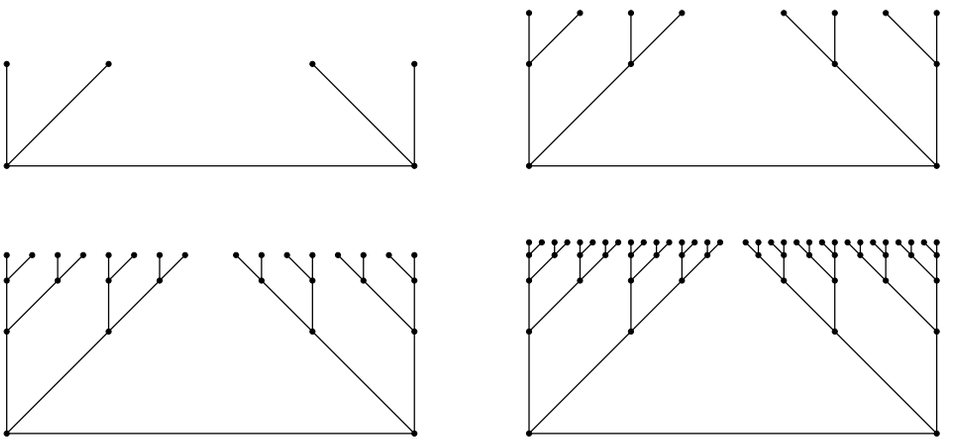

Figure 8. The basic building blocks are pairs of binary trees. Shown are the trees $\widehat{T}_1$, $\widehat{T}_2$, $\widehat{T}_3$ and $\widehat{T}_4$.

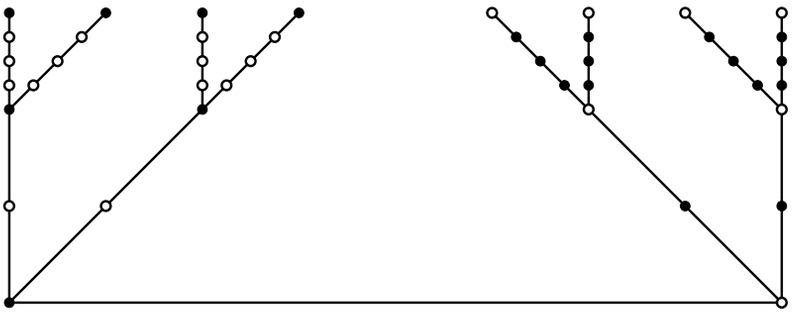

Figure 9. We add vertices to $\widehat{T}_j$ to get T_j. The jth level is divided into 2^j equal subedges by adding extra vertices. We illustrate only the $j=2$ case, since its hard to see individual vertices at higher levels; most of our figures will not show these vertices at all, but their presence is essential to the construction.

How many edges are in T_j? How many sides? If we simply count the edges in T_2 of Figure 9, for example, we get one base edge, 8 level-1 edges, 32 level-2 edges, and, in general, 2^{2j+1} level-j edges. So the number of edges is

$$1+\sum_{k=1}^{j} 2^{2k+1} = -1+2\sum_{k=0}^{j} 4^k = \frac{2}{3}(4^{j+1}-1)-1.$$

Normally, the number of sides would be twice the number of edges, but for our purposes, we only want to count a side of T_j if it is accessible from the interior of R_j, the convex hull of T_j. Thus we have to subtract the "inaccessible" sides belonging to the bottom and sides of R_j. After a little arithmetic, this gives

$$N_j = \left(\frac{4}{3}(4^{j+1}-1)-2\right) - \left(1+2\sum_{k=1}^{j} 2^k\right) = \frac{4}{3}(4^{j+1}-1)+1-2^{j+2}.$$

The first few values are 13, 69, 309, ... Because of symmetry, we know that the answer is odd and less than 4^j.

The next step is to introduce "clipped" versions of the trees T_j and their convex hulls. We let $T_j^{l,k}$ be the tree T_j with the top l levels of the the left-hand side removed, together with all the other edges that are disconnected from the base. We also remove the top k levels of the right-hand side. Let $R_j^{l,k}$ be the convex hull of the remaining tree. See Figure 10. If $l=j$ then we say the tree has been clipped down to its root. The number of sides in $T_j^{l,k}$ is

$$N_{j,l,k} = N_j - (2^j + ... + 2^{j-l+1}) - (2^j + ... + 2^{j-k+1}) \geqslant N_j - 2^{j+2} + 2.$$

The exact number is not important, but we will need that it is odd and comparable to 4^j (to get oddness, it is important to remember that this is the tree T_j, not $\widehat{T}_j$, so there are an even number of edges on T_j in each level along the left and right sides of R_j).

Note that $R_j \backslash T_j$ has $2^{j+1}-1$ connected components, of which 2^j are triangles. Similarly $R_j^{l,k} \backslash T_j^{l,k}$ has $2^j - 2^{l-1} - 2^{k-1}$ triangular components. If $j \geqslant 2$, the number of triangular components is between 2^{j-1} and 2^j regardless of the values of l and k, hence the number is comparable to 2^j. This is also true for $j=1$ unless $j=l=k=1$, in which case there are no such components. Each of these triangular components has exactly one vertex that is not on the top edge of R_j. We call this the bottom vertex of the component.

So far, we have built trees that have an exponentially growing odd number of sides. We want to be able to achieve any odd number, and to do this, we will add edges to our clipped trees. Suppose we are given an odd, positive integer m and define the level of

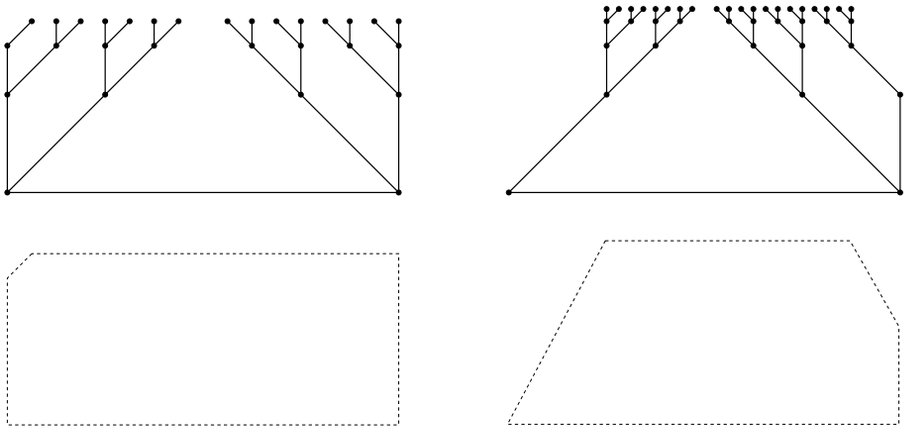

Figure 10. The clipped trees $T_3^{1,0}$ and $T_4^{4,3}$ are shown in solid lines. On the bottom are the convex hulls $R_3^{1,0}$ and $R_4^{4,3}$.

m as the value of j such that $N_j \leqslant m < N_{j+1}$, where we set $N_0 = 1$ and N_j is defined as above.

Suppose we are also given non-negative integers l and k that are both less than the level j of m. We will add edges to the clipped tree $T_j^{l,k}$ so that the total number of edges is m.

First suppose $j \geqslant 2$. Then there are $\sim 2^j$ triangular components of $R_j^{l,k} \setminus T_j^{l,k}$, and we add a segment connecting the center of the pth triangle to its bottom vertex and divide it into n_p equal subsegments. We call such a segment a "spike". See Figure 11. We choose the integers $\{n_p\}_p$ so that

$$2 \sum_p n_p = m - N_{j,l,k} \quad \text{and} \quad n_p = O(2^j),$$

where the constant is allowed to depend on l and k (eventually both of these will be chosen to be $O(1)$, so the constant above will also be $O(1)$). If $j = 1$ and $l = 0$ or $k = 0$ then there is at least one triangular component where we can add a spike. If $j = 1$ and $l = k = 1$, then instead of adding a spike, use a simple folding in place of $T_1^{1,1,}$.

Now we are ready to define the domain $W \subset \mathbb{H}_u$ associated with the partition $\mathcal{J}$ of $\mathbb{R}$. Suppose $J \in \mathcal{J}$ and let m be its length (an odd, positive integer). Let j be the level of m and let j_1 and j_2 be the levels of the elements of $\mathcal{J}$ that are adjacent to J and to its left and right respectively. Let

$$l = \max\{0, j - j_1\} \quad \text{and} \quad k = \max\{0, j - j_2\},$$

and associate with J the tree $T_{j,m}^{l,k}$. The indices l and k have been chosen so that when two intervals are adjacent, and the corresponding trees have different levels, then the

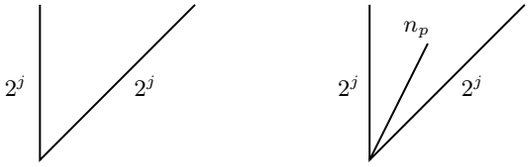

Figure 11. Spikes are added to some vertices of the tree to bring the total number of sides up to m. Adding zero spikes is allowed. These extra spikes will often be omitted from our pictures.

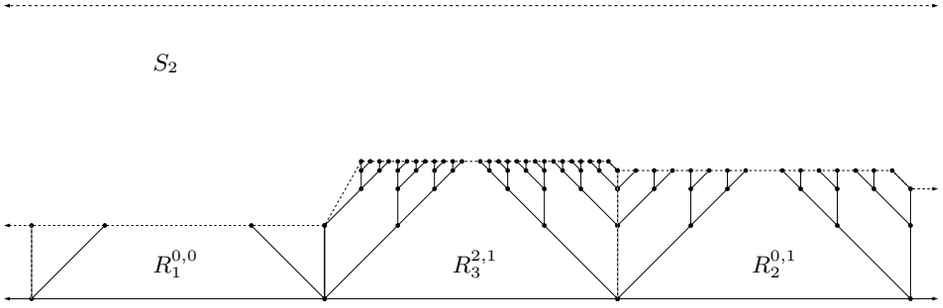

Figure 12. We form a variable width strip, S_2, by taking the union of convex hulls $R_{j,m}^{l,k}$ corresponding to our partition (in the picture we ignore m). The lower boundary of S_2 is a Lipschitz graph. The solid lines indicate the union of trees Γ and $W=\mathbb{H}_u\setminus\Gamma$.

higher tree has been clipped to match the level of its lower neighbor. Thus the union of the clipped convex hulls $\bigcup R_j^{l,k}$ has an upper edge that is a Lipschitz graph γ (the graph coincides with the real line on intervals where we use a simple folding). The region above Γ and below height 2 is a variable width strip that we denote S_2.

If m has level $\geqslant 1$, then inside the copy of $R_j^{l,k}$ with base J we place a copy of the tree $T_{j,m}^{l,k}$ and remove this tree from the upper half-plane. If the m has level 0, or we are in the case when $j=1=k$ discussed earlier, $R_j^{l,k}$ is a line segment on $\mathbb{R}$ and we remove a diagonal line segment divided into $\frac{1}{2}(m-1)$ edges; above these intervals the map will be a simple folding of size m. Doing one of these steps for every element of the partition defines the simply connected region $W=\mathbb{H}_u\setminus\Gamma$. See Figure 12.

6. The folding map: building the triangulation

In the previous section we built a domain $W\subset\mathbb{H}_u$. In this section we build the map ψ. As described in the introduction, we build our quasiconformal maps by giving compatible triangulations of the domain and range, and mapping corresponding triangles to each other by an affine map. Up to Euclidean similarity, only a finite number of different pairs of triangles will be used (depending only on the number M in the lemma), so the

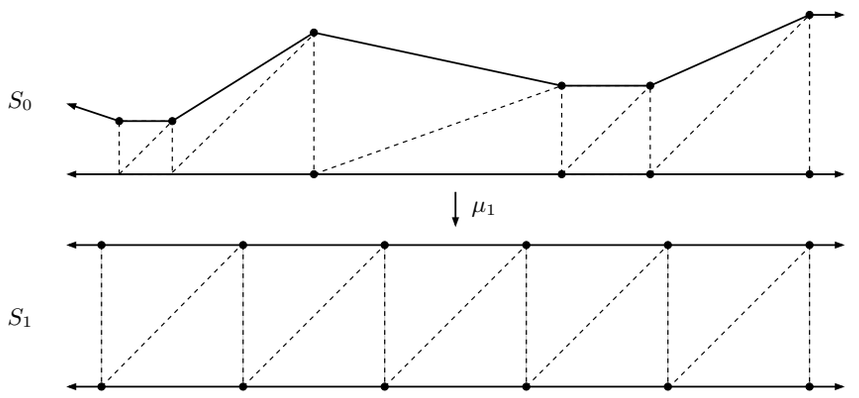

Figure 13. The map μ_1. It is quasiconformal because the trapezoids have heights comparable to their bases (because adjacent intervals have lengths comparable within a factor of M).

maximum dilatation of our map is bounded. Hence the map will be quasiconformal with constant depending only on M.

Although we do not need an explicit bound for our purposes, it is easy to compute the quasiconformal constant of an affine map between triangles. Conformal linear maps can be used to put the triangles in the form $\{0,1,a\}$ and $\{0,1,b\}$, $a,b{\in}\mathbb{H}_u$, and the affine map is then

$$f(z)=\alpha z+\beta\bar{z},$$

where $\alpha{+}\beta{=}1$ and $\beta{=}(b{-}a)/(a{-}\bar{a})$. Then the dilatation is

$$\mu_f=\frac{f_{\bar{z}}}{f_z}=\frac{\beta}{\alpha}=\frac{b-a}{b-\bar{a}},$$

which is the pseudo-hyperbolic distance between a and b in the upper half-plane.

The map ψ is defined as a composition of several simple maps and a more complicated one. Given two adjacent intervals J_k and J_{k+1} of our partition $\mathcal{J}$ with common endpoint x_k, let $h_j{=}\min\{\ell(J_k),\ell(J_{k+1})\}$ be the length of the shorter one and let $z_k{=}x_k{+}ih_k$. Form an infinite polygonal curve by joining these points in order, and let S_0 be the region bounded by this curve and the real axis. The vertical crosscuts at the points x_k cut the region into trapezoids and because of our assumption about the lengths of adjacent elements of $\mathcal{J}$ being comparable, only a compact family of trapezoids occur. See the top half of Figure 13.

It is easy to quasiconformally map S_0 to the strip

$$S_1=\{x{+}iy:0<y<2\}$$

by mapping each trapezoid to a square of side length 2 (cut each trapezoid into triangles by a diagonal and map these linearly to the right triangles obtained by cutting the square by a diagonal). Denote this map by μ_1. See Figure 13.

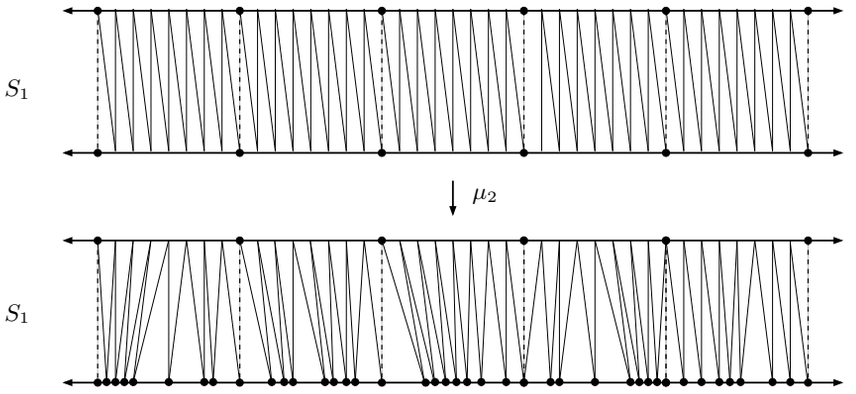

Figure 14. The map μ_2. It is quasiconformal because it is bi-Lipschitz on the lower boundary and the identity on the upper boundary.

Next we define a map $\mu_2\colon S_1 \to S_1$ that is the identity on the top edge of S_1 and bi-Lipschitz on the bottom edge. Such a map clearly has a bi-Lipschitz extension to the interior of the strip, so we only have to define the map on the lower boundary. See Figure 14. Suppose I is an interval of length 2 on the bottom edge of S_1 that corresponds to a an interval $J \in \mathcal{J}$ of length m and that $T_{j,m}^{l,k}$ is the corresponding clipped tree. If this tree is a simple folding, we just take μ_2 to be the identity on I. Otherwise, project the degree-1 vertices of $T_{j,m}^{l,k}$ vertically onto I. These points partition I into subintervals $\{I_p\}_p$ that correspond one-to-one to the components $\{V_p\}_p$ of $V = R_{j,m}^{l,k} \setminus T_{j,m}^{l,k}$. If V_p has m_p sides, divide I_p into m_p equal subintervals. This gives a partition of I into $m = \sum_p m_p$ intervals (of possibly different sizes). The map μ_2 just maps the partition of I into m equal-length intervals to this "unequal" partition. The map is bi-Lipschitz because each interval in the "unequal" partition has length comparable to $|I|/m$ (by the calculations of the previous section, if m has level $j \geqslant 1$ then $m \simeq 4^j$, there are $\simeq 2^j$ components of V and each contains $\simeq 2^j$ sides).

Next we define a variable width strip S_2 whose upper boundary is $\{x+iy : y=2\}$ and whose lower boundary is the upper envelope γ of the union of the regions $R_{j,m}^{l,k}$. We let $\mu_3\colon S_1 \to S_2$ be a bi-Lipschitz map that is the identity on the top boundary of S_2 and agrees with vertical projection onto γ on the bottom edge (again easy to define using triangulations; see Figure 15).

The final step is to define a quasiconformal map $\mu_4\colon S_2 \to S_1 \cap W$ that is the identity on the top edge of S_2 and maps each element of $\mathcal{P}$ linearly to a side of W. Building this map will occupy the rest of this section. Assuming we can do this, then we set ψ to be

$$S_0 \xrightarrow{\mu_1} S_1 \xrightarrow{\mu_2} S_1 \xrightarrow{\mu_3} S_2 \xrightarrow{\mu_4} W \xrightarrow{\mu_1^{-1}} S_0$$

in S_0 and let it be the identity in $\mathbb{H}_u \setminus S_0$. See Figure 16. All the conclusions of Lemma 5.1

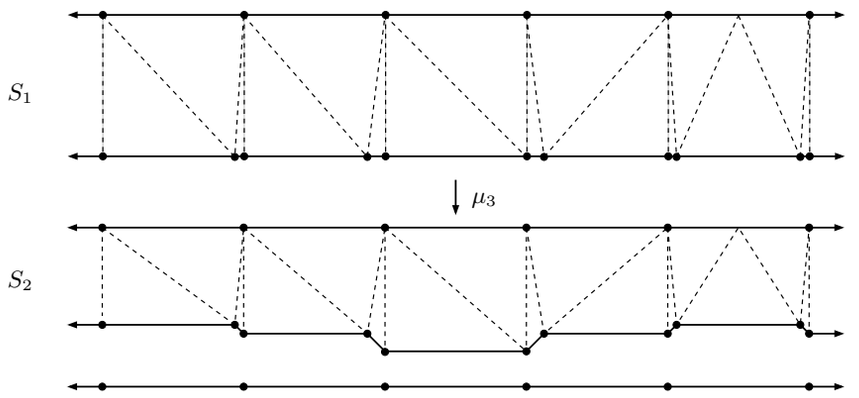

Figure 15. The map μ_3. It is quasiconformal because the lower boundary of S_2 is a Lipschitz graph.

follow directly from the construction.

The final step is to construct the map μ_4. Let I be an interval of length 2 corresponding to some $J\in\mathcal{J}$ and let $Q\subset S_1$ be the 2×2 square with base I. The map μ_4 is the identity above S_2, so we only need to define it inside each such Q so that it is the identity on $\partial Q\cap S_2$ (then the definitions on different squares will join to form a quasiconformal map on S_2).

If $W\cap Q$ is a simple folding, we have already seen how to define μ_4 in Figure 7. Otherwise, suppose that Q contains the convex hull $R=R_j^{l,k}$ of a the tree $T=T_{j,m}^{l,k}$. Let $R'=R_j$ be the "unclipped" version of R. As noted earlier, $\partial R\setminus T$ consists of intervals, and each interval I_p has been partitioned into m_p equal-length intervals where m_p is the number of sides of the corresponding component of $R\setminus T$. The interval I_p is horizontal unless it is the leftmost or rightmost interval, in which case it may be sloped (the "clipped" part of R).

For horizontal intervals I_p we let $Q_p\subset Q\setminus R$ be the square with base I_p. For sloped intervals we let Q_p denote the triangular component of $R'\setminus R$ containing the interval. Let W_p be the component of $R\setminus T$ with I_p as its top edge (see Figure 17). We want to define $\mu_4\colon Q_p\to U_p=Q_p\cup W_p$ to be quasiconformal, to be the identity on $\partial Q_p\setminus\overline{W}_p$, and to map each interval in our partition of I_p to a side of W_p. We call this a "filling map", since it fills W_p. There are a number of different cases, but each can be constructed with a simple picture.

Figure 17 shows the four types of components W_p that have to be considered:

(1) top triangles;
(2) corner triangles;
(3) parallelograms;
(4) the center triangle.

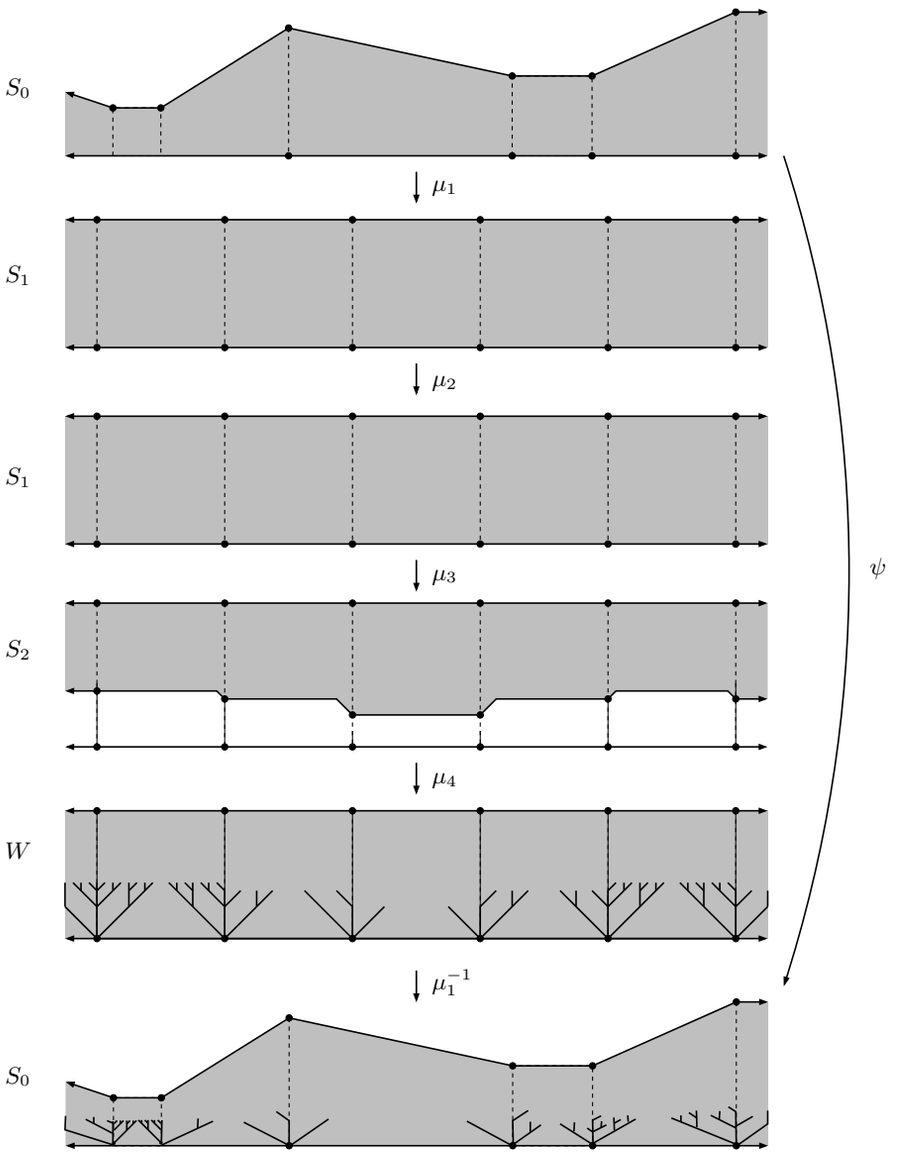

Figure 16. The maps $S_0 \xrightarrow{\mu_1} S_1 \xrightarrow{\mu_2} S_1 \xrightarrow{\mu_3} S_2 \xrightarrow{\mu_4} W \xrightarrow{\mu_1^{-1}} S_0$ define ψ.

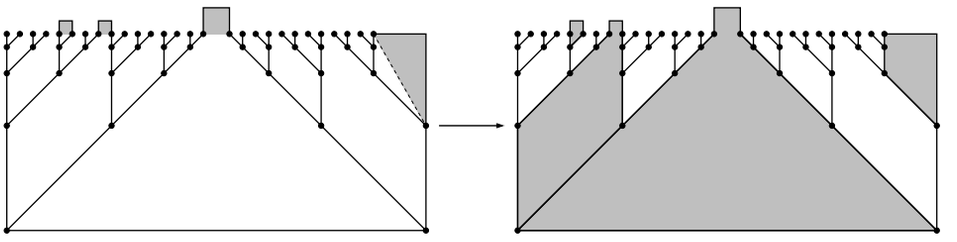

Figure 17. Some examples of filling maps. In each case, a square is mapped to the union of itself and the region below it bounded by the tree. The picture omits a large number of vertices on the upper levels and the "spikes" that were added to the triangular components. For a clipped tree, there is an additional case covering the leftmost and rightmost intervals.

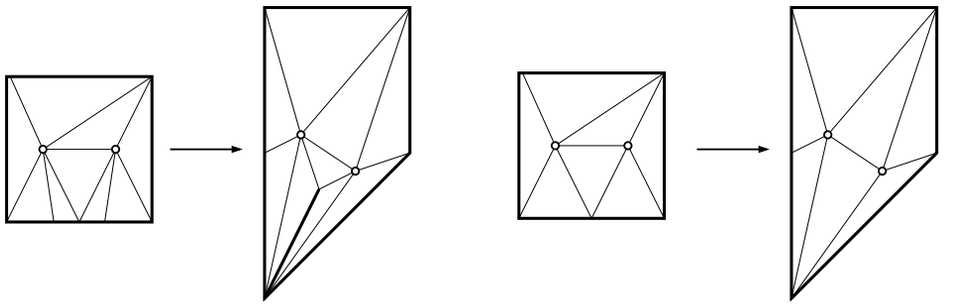

Figure 18. The left map is used for the small triangular components with a slit. The four intervals on the bottom of the square have relative lengths 2^j, n_j, n_j, 2^j, so that the maps send the correct number of vertices onto each segment of the tree. The right side shows the filling map when there is no slit (i.e., $n_j{=}0$).

In each case, the map from Q_p to U_p is specified by drawing compatible triangulations of the two regions and then taking the piecewise affine map between these triangulations.

Figure 18 shows the triangulations for the top triangles. These triangles may or may not contain a spike, so both situations are illustrated. The placement of the vertices on the bottom edge of Q_p is determined by the number of sides on the spike, but the map is clearly uniformly quasiconformal as long as the number of these edges is at most a fixed fraction of m_p (this is true by the estimate $m_p{=}O(2^j)$ discussed in the previous section).

Figure 19 shows the triangulation for the corner triangles (these only occur if the corresponding tree was clipped). This is a very simple map that just moves points along the interval I_p; the partition of I_p is in equal-length intervals, but the sides of T get smaller as we approach the top of T and this map makes the correction. The quasiconformal constant depends on the number of levels (l or k) that have been clipped, but this is bounded depending only on the number M in the lemma (if adjacent intervals of $\mathcal{J}$ have comparable lengths, then the levels of adjacent trees differ by a uniform additive constant, so the amount of clipping is uniformly bounded). This is the only part of the

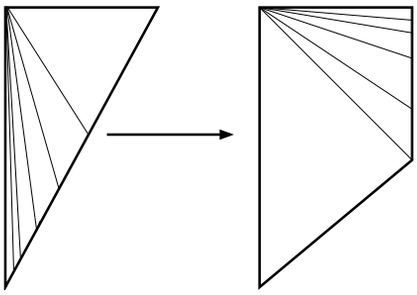

Figure 19. The filling map for the clipped ends, which just moves points along the diagonal edge, so the qth level edge gets 2^q points. This distortion depends on the clipping indices, l and k, but these are uniformly bounded, so the total distortion is too.

construction where the quasiconformal constant of ψ depends on M.

Figure 20 shows the triangulations of the parallelogram components. Each such component U_p has a fixed top piece (a square), a bottom piece (a triangle) and a variable number of middle pieces (all similar to the same trapezoid). We decompose Q_p into the same number of nested pieces as shown and map each piece to its corresponding image using the triangulations shown. Since only a finite number of pieces are used (up to Euclidean similarities), the quasiconformal constant is uniformly bounded.

Figure 21 shows the analogous picture for the large central component. The top piece is exactly the same as for the parallelogram components, so we only illustrate the triangulations for the middle and bottom sections. This figure finishes our description of the map $\mu_4 \colon S_2 \to S_1 \cap W$; this completes the proof of Lemma 5.1 and hence of Theorem 1.1.

7. Asymptotic values and high-degree critical points

The construction described in Theorem 1.1 does not allow finite asymptotic values or critical points with arbitrarily high degree. However, these features are important in several applications, so in this section we describe how to extend the construction to include them. Note that no extra "hard work" is needed; we simply supplement the early construction by allowing some complementary components where no quasiconformal folding takes place.

In Theorem 1.1 each complementary component of T is mapped to $\mathbb{H}_r$. In our generalization, the tree T is replaced by a connected graph whose complementary components are each mapped to one of three possible standard domains:

(1) the unit disk, $\mathbb{D}$;
(2) the left half-plane, $\mathbb{H}_l$;
(3) the right half-plane, $\mathbb{H}_r$.

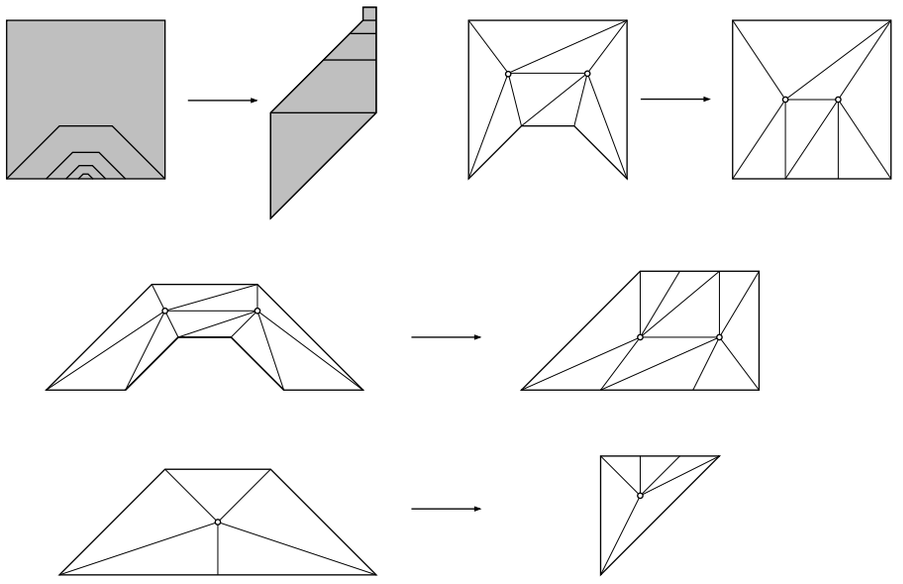

Figure 20. This map is used for all the "parallelogram" components. The base of the square is divided into intervals of relative lengths $2^j, 2^{j-1}, ..., 2^{k+1}, 2^k, 2^k, 2^{k+1}, ... 2^{j-1}, 2^j$, to insure the correct number of vertices are sent to each level of the tree.

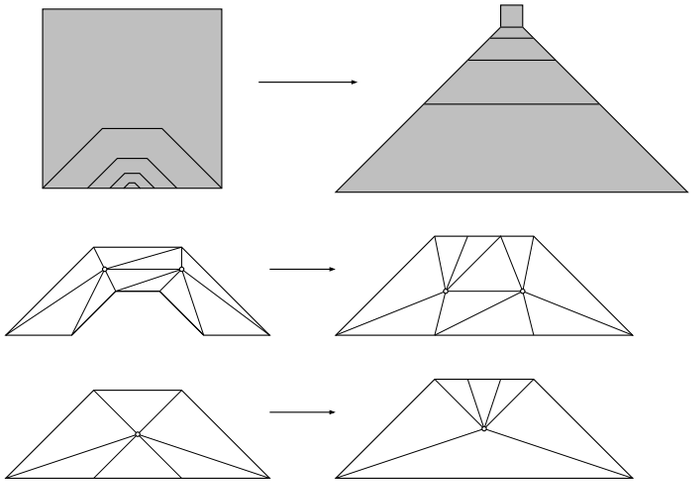

Figure 21. This is the map for the central component. The top piece is mapped as in the previous case, so we only illustrate the middle and bottom maps. The base of the square is divided into intervals of relative lengths $2^j, 2^{j-1}, ..., 4, 2, 2, 2, 4 ... 2^{j-1}, 2^j$, to insure the correct number of vertices are sent to each level of the tree.

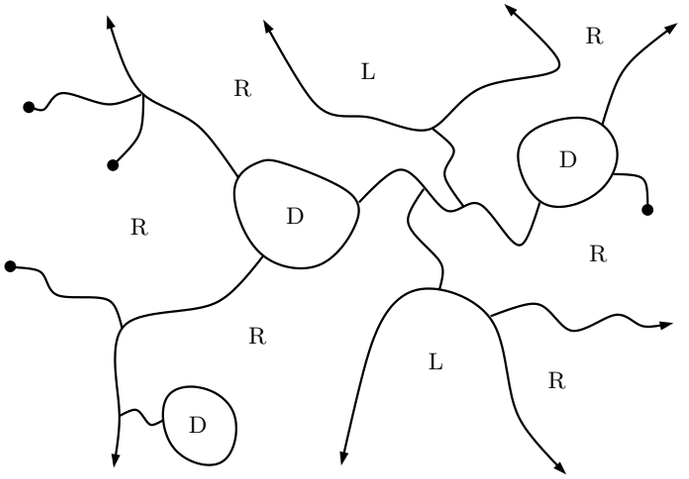

Figure 22. To allow asymptotic values and high-degree critical values we replace the tree T by a graph that divides the plane into three types of components: D-components that are bounded Jordan domains, L-components that are unbounded Jordan domains and R-components that are unbounded simply connected domains (they need not be Jordan). D-components and L-components may only share an edge with an R-component and QC folding will only be applied on the R-components.

We shall refer to these as D-components, L-components and R-components, respectively. If only L- and R-components are used then the graph T is still a tree. Theorem 1.1 corresponds to the special case when every complementary component is an R-component. We do not allow D- and L-components to share an edge.

Each component comes with a length-respecting quasiconformal map η to its corresponding standard version and each standard domain has a map σ into the plane that plays the role of cosh in Theorem 1.1. These are chosen so that $g{=}\sigma{\circ}\,\eta$ defines a quasiregular map on the plane that can be converted to an entire function $f{=}g{\circ}\phi$ by an application of the measurable Riemann mapping theorem to find the appropriate quasiconformal ϕ. Before stating the theorem, we discuss each type of component.

D-components. Ω is bounded and $\partial\Omega$ is a closed Jordan curve that is the union of a finite number of edges of T, say d. We are given a length-respecting (on the boundary) quasiconformal map $\eta\colon\Omega{\to}\mathbb{D}$ and we assume the n vertices on $\partial\Omega$ map to the nth roots of unity on the circle. The map $\sigma\colon\mathbb{D}{\to}\mathbb{D}$ is $z{\mapsto}z^d$ followed by a quasiconformal map $\varrho\colon\mathbb{D}{\to}\mathbb{D}$ that is the identity on $\partial\mathbb{D}$. We often take ϱ to be the identity, and this gives a critical point of degree d with critical value 0. If a critical value a is desired, then ϱ is chosen so $\varrho(0){=}a$. If $|a|{<}\frac{1}{2}$, then ϱ can be chosen to be conformal on $\{z\colon|z|{<}\frac{3}{4}\}$, so in this case, the dilatation of ϱ is supported on $\{z\colon\frac{1}{4}{<}|z|{<}1\}$. Thus, in all cases, the dilatation of σ is bounded by $O(|a|)$ and is supported on $\{z\colon1{-}(\log 4)/d{<}|z|{<}1\}$.

L-components. Here Ω is an unbounded Jordan domain and we are given a length-respecting quasiconformal $\eta\colon\Omega\to\mathbb{H}_l$. The map $\sigma\colon\mathbb{H}_l\to\mathbb{D}\setminus\{0\}$ is just $z\mapsto\exp(z)$. This gives a component with finite asymptotic value 0. If a different asymptotic value a with $|a|<\frac{1}{2}$ is desired, we post-compose this map with a quasiconformal map $\varrho\colon\mathbb{D}\to\mathbb{D}$ such that $\varrho(0)=a$ and ϱ is the identity on $\partial\mathbb{D}$ (just as for critical values for D-components).

R-components. This is what we used in Theorem 1.1. Here Ω is simply connected and unbounded and we are given a length-respecting quasiconformal map $\eta\colon\Omega\to\mathbb{H}_r$. The boundary may be a tree instead of a Jordan curve. In Theorem 1.1, we took $\sigma=\cosh$, but now we have to allow more general maps. Under the map $\tau_j^{-1}\colon\mathbb{H}_r\to\Omega_j$, each interval I in the partition is mapped to one side of an edge e of T and either the other side of this edge also faces the same component Ω_j, or it faces a different component Ω_k, $k\neq j$. In the latter case, the second component Ω_k could be a D-, L- or R-component.

We divide the intervals in our integer partition of $\partial\mathbb{H}_r$ into two types. We say the interval is *type*-1 if the corresponding opposite side of $\tau_j^{-1}(I)$ belongs to an R-component; this can either be the same component Ω_j or a different component Ω_k. We say the interval is *type*-2 if the other side of $\tau_j^{-1}(I)$ faces a D-component or an L-component (which is necessarily a different component of Ω). We denote these two collections of intervals on $\partial\mathbb{H}_r$ by $\mathcal{J}_1^j$ and $\mathcal{J}_2^j$. We now choose a map $\mathbb{H}_r\to\mathbb{C}$ that equals cosh on the type-1 intervals, equals exp on the type-2 intervals and equals cosh far from $\partial\mathbb{H}_r$. More precisely, we have the following result.

LEMMA 7.1. (exp-cosh interpolation) *There is a quasiregular map $\nu_j\colon\mathbb{H}_r\to\mathbb{C}\setminus[-1,1]$ so that*

$$\nu_j(z)=\begin{cases}\cosh(z), & \text{if } z\in J\in\mathcal{J}_1^j,\\ \exp(z), & \text{if } z\in J\in\mathcal{J}_2^j,\\ \cosh(z), & \text{if } z\in\mathbb{H}_r+1=\{x+iy:x>1\}.\end{cases}$$

The quasiconstant of ν_j is uniformly bounded, independent of all our choices.

Proof. The proof is basically a picture; see Figures 23 and 24. Suppose J is one of our partition intervals and let $R=[0,1]\times J\subset\mathbb{H}_r$. The cosh map sends R into a topological annulus bounded by the unit circle and the ellipse $E=\{x+iy:(x/s)^2+(y/t)^2=1\}$, where $x=\frac{1}{2}(e+1/e)$ and $y=\frac{1}{2}(e-1/e)$. The left side of R maps to the unit circle, the right side maps to E, and the top and bottom edges of R map to the real segment $[1,e]$. Let U be the region bounded by the ellipse and $V=U\setminus\mathbb{D}$ be the annular region.

Now define a quasiconformal map $\phi\colon V\to U$ that is the identity on E and on $[1,e]$, but that maps $\{z\colon|z|=1\}$ onto $[-1,1]$ by $z\to\frac{1}{2}(z+1/z)$ (this is just the Joukowsky map that conformal maps the exterior of the unit circle to the exterior of $[-1,1]$ and identifies

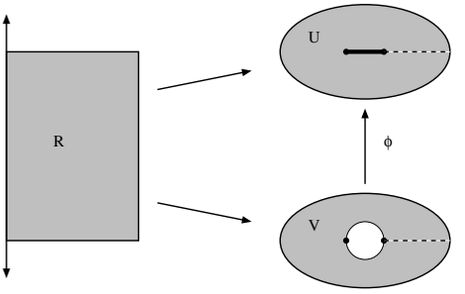

Figure 23. The cosh map sends the rectangle R to an ellipse minus the unit disk. On some rectangles we modify it to map to the ellipse minus $[-1,1]$.

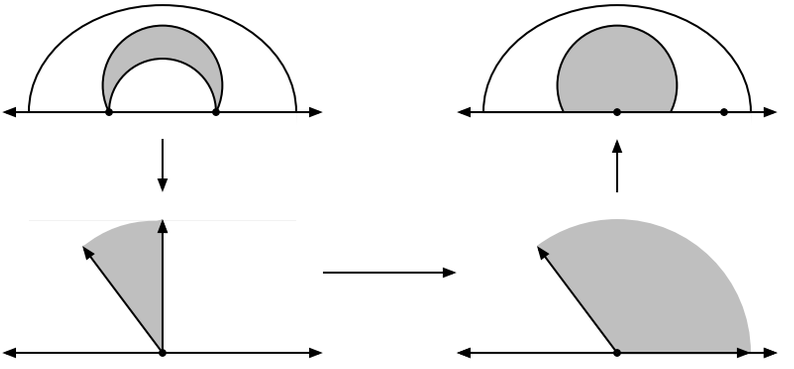

Figure 24. We show only the construction in the upper half-plane; it is defined symmetrically in the lower half-plane. The region V contains a crescent with vertices at ± 1 as shown. The crescent can be Möbius mapped to a sector which can be quasiconformally mapped to a larger sector by fixing radii and and expanding arguments. Mapping back by another Möbius transformation gives the desired quasiconformal map from V to U.

complex conjugate points). This map can clearly be extended from the boundary of V to the interior as a quasiconformal map. See Figure 24.

In $\mathbb{H}_r+1$ and in rectangles corresponding to $J\in\mathcal{J}_1^j$, we set $\nu(z)=\cosh(z)$. In the rectangles corresponding to elements of $\mathcal{J}_2^j$ we let $\nu(z)=\phi(\cosh(z))$. This clearly has the properties stated in the lemma. The map can be visualized as a map from $\mathbb{H}_r$ to a Riemann surface with sheets of the form either $\mathbb{C}\backslash[-1,1]$ or $\mathbb{C}\backslash\overline{\mathbb{D}}$ attached along $[1,\infty)$ and chosen according to the type of the corresponding partition element. See Figures 25 and 26. □

THEOREM 7.2. *Let T be a bounded-geometry graph and suppose τ is conformal from each complementary component to its standard version. Assume that* D- *and* L-*components only share edges with* R-*components. Assume that τ on a* D-*component with n edges maps the vertices to n-th roots of unity and on* L-*components it maps edges to*

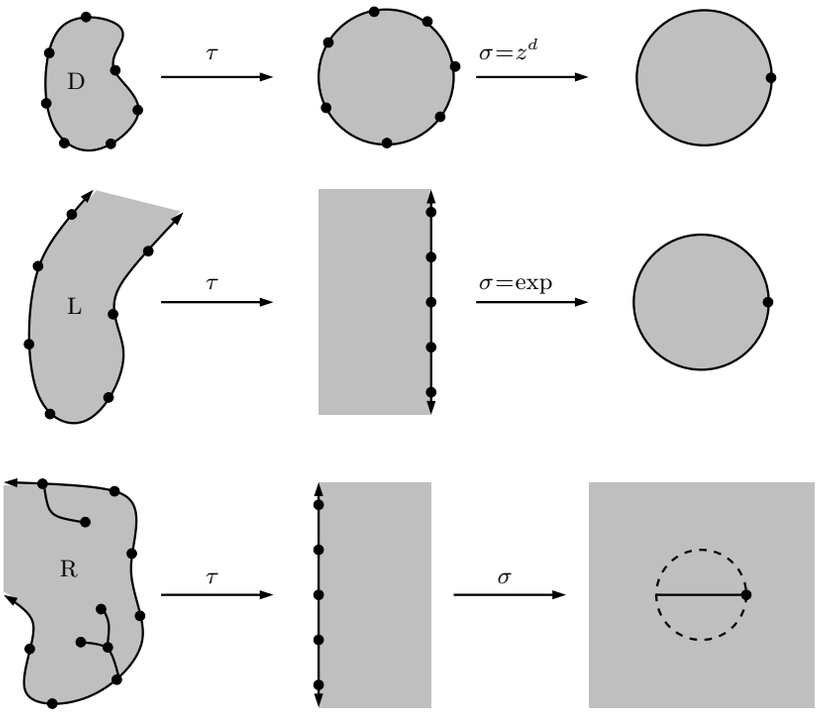

Figure 25. Each of the three types of components is mapped to its standard domain ($\mathbb{D}$, $\mathbb{H}_l$ or $\mathbb{H}_r$) and then followed by a covering map ν. For R-components ν may map onto a Riemann surface instead of a covering of a planar domain. See Figure 26 for more details about the R-components.

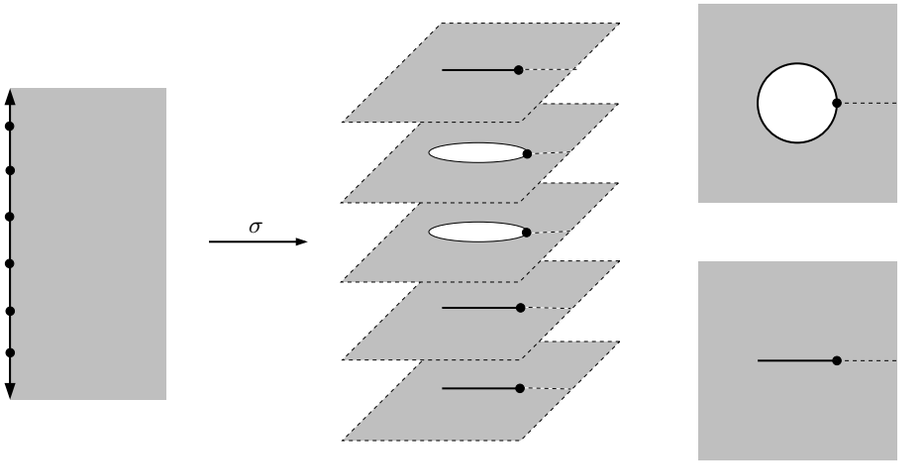

Figure 26. R-components are attached to other R-components using $\cosh(z)$ and are attached to D- and L-components using $\exp(z)$. The corresponding map ν is a combination of these two boundary values and can be visualized as mapping $\mathbb{H}_r$ onto a Riemann surface made by attaching copies of $\{z{:}|z|{>}1\}$ and $\mathbb{C}\backslash[-1,1]$ along $(1,\infty)$.

intervals of length 2π *on* $\partial\mathbb{H}_l$ *with endpoints in* $2\pi i\mathbb{Z}$. *On* R*-components assume that the* τ*-sizes of all edges are* $\geqslant 2\pi$. *Then there is an entire function* f *and a quasiconformal map* ϕ *of the plane so that* $f\circ\phi=\nu\circ\tau$ *off* $T(r_0)$. *The only singular values of* f *are* ± 1 (*critical values coming from the vertices of* T) *and the critical values and singular values assigned by the* D- *and* L*-components.*

Given our previous arguments, there is hardly anything to say about the proof of this. We apply the folding construction to each right half-plane component and define a quasiregular map on each such component whose boundary values match the function on the other side of every edge (either the given maps for D- and L-components or a folded map for an R-component). Then apply the measurable Riemann mapping theorem as before.

8. Lower bounds for the τ-size of an edge

The remainder of the paper deals with various applications of Theorems 1.1 and 7.2. Aside from any intrinsic interest, the examples are intended to show that applying our results follows an easy procedure:

(1) Draw a picture of the graph T and label the complementary components as D-, L- and R-components.

(2) Place vertices so that the D- and L-components map to "evenly spaced" points in the standard domain under a conformal or uniformly quasiconformal map.

(3) Add extra points, if necessary, to insure the tree has bounded geometry. We may also add extra vertices to make the neighborhood $T(r_0)$ small, while maintaining bounded geometry.

(4) Choose τ on each R-component so that the τ-size of every edge is $\geqslant\pi$.

For the examples we will give, the first three steps are always easy; only the last one requires some calculation. Moreover, we can usually replace τ by a positive multiple of itself on any component, so it usually suffices to prove that the τ-sizes of edges have a positive lower bound. In this section we will show how to do this using simple estimates of the hyperbolic metric on the components of $\Omega=\mathbb{C}\setminus T$.

Suppose that Ω is a complementary component of a bounded-geometry tree T. Assume that $\tau\colon\Omega\to\mathbb{H}_r$ is conformal and fixes ∞ and let $\mathcal{I}=\{I_j\}_j$ be the corresponding partition of $\partial\mathbb{H}_r$. Associated with each $I\in\mathcal{I}$ is a hyperbolic geodesic γ_I in $\mathbb{H}_r$ with the same endpoints as I; this is just a semicircle with diameter $\ell(I)$. Let z_0 be the rightmost point of γ_0 and let γ_∞ be the horizontal ray connecting z_0 to ∞ in $\mathbb{H}_r$. Let z_j, $j\neq 0$, be the closest point of γ_j to γ_∞ and let $x_j\in\gamma_\infty$ be the closest point to γ_j.

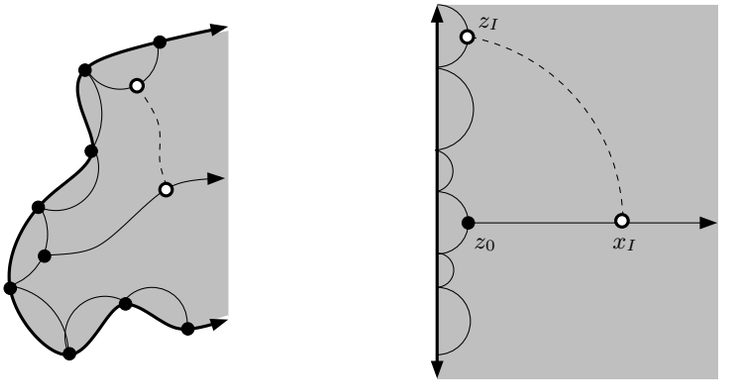

Figure 27. The τ-size of an edge can be estimated using hyperbolic geometry. We associate with each partition interval the hyperbolic geodesic with the same endpoints. An image interval has Euclidean length bounded below if the hyperbolic distance from z_I to x_I is less than the distance from x_I to z_0 plus a bounded factor.

A simple computation shows that $\ell(I_j)\geqslant\ell(I_0)$ if

$$\varrho(x_j,\gamma_j)\leqslant\varrho(x_j,\gamma_0), \tag{8.1}$$

where ϱ denotes the hyperbolic metric. Thus to prove a lower bound for the τ-size of edges of T, it is enough to verify (8.1). By the conformal invariance of the hyperbolic metric, we can often check this directly on Ω. Indeed, in many examples, we can verify stronger estimates

$$\varrho(x_j,\gamma_j)\leqslant\lambda\varrho(x_j,\gamma_0) \tag{8.2}$$

for some $0\leqslant\lambda<1$, or

$$\varrho(x_j,\gamma_j)\leqslant C \tag{8.3}$$

for some $C<\infty$.

We can interpret (8.1) in terms of harmonic measure. For a partition element I_j, $j\neq0$, let I_j^∞ be the component of $\partial\mathbb{H}_r\setminus I_j$ not containing I_0. Then $\ell(I_j)\gtrsim\ell(I_0)$ if

$$\omega(z_0,I_j,\mathbb{H}_r)\gtrsim\omega(z_0,I_j^\infty,\mathbb{H}_r)^2.$$

Here ℓ denotes Euclidean length on $\partial\mathbb{H}_r$. By conformal invariance of harmonic measure, it is enough to check this for the corresponding arcs on $\partial\Omega$, which is often easy to do. Indeed, in most of the examples we will see, we will have the much stronger estimate

$$\omega(z_0,I_j,\mathbb{H}_r)\gtrsim\omega(z_0,I_j^\infty,\mathbb{H}_r),$$

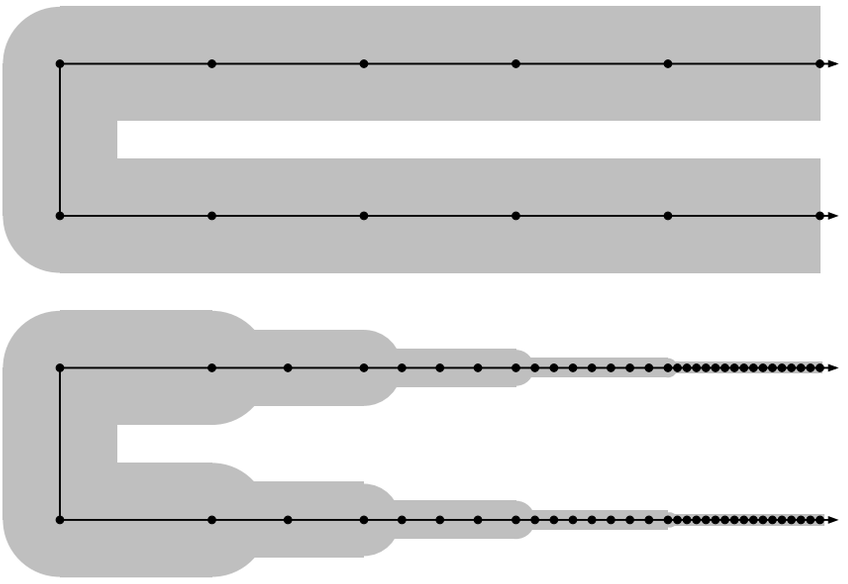

Figure 28. The boundary of a half-strip is a bounded-geometry tree if we use equally spaced vertices, but the τ-images of the edges grow exponentially since (8.3) holds (for the half-strip $\tau=\sinh$). We can let edge lengths decay exponentially and still have bounded geometry, large τ-sizes but a much smaller $T(r_0)$. Hence the correction map ϕ is "more" conformal with the new vertices.

which corresponds to estimate (8.3) for the hyperbolic metric. In either case, $\ell(I_j)$ grows exponentially with $|j|$. When this happens, we can often add extra vertices to the edges of T while maintaining both the bounded-geometry condition (only the comparable lengths of adjacent edges needs to be re-checked; the other conditions are automatically fulfilled) and the large τ-size condition. Adding vertices means the set $T(r_0)$ becomes smaller, and hence the "correcting" map ϕ is conformal on a larger set. See Figure 28. If we can shrink the area of $T(r_0)$ to zero, while keeping the dilatation of ϕ bounded, then ϕ converges to the identity.

Why is this important? We build a quasiregular function g with a certain property and want to know if the entire function $f=g\circ\phi$ has the same property. For a general quasiconformal map ϕ we cannot say much more than it is bi-Hölder, i.e.,

$$\frac{1}{C}|z-w|^{1/\alpha} \leqslant |\phi(z)-\phi(w)| \leqslant C|z-w|^{\alpha}$$

for some $\alpha\in(0,1]$. However, if ϕ is conformal except on a small set, we can say much more. The logarithmic area of a planar set is defined as

$$\operatorname{logarea}(E) = \int_E \frac{dx\,dy}{x^2+y^2}.$$

A well-known result of Teichmüller and Wittich (e.g., [27, Theorem 7.3.1], [47], [49]) says that if a quasiconformal map ϕ is conformal except on a set of finite logarithmic area near infinity, then ϕ is asymptotically conformal, i.e., $\lim_{|z|\to\infty} |\phi(z)|/|z|$ exists and has a finite, non-zero value. In many cases of interest, we know not just that the logarithmic area is finite but that it decays exponentially, e.g.,

$$\operatorname{logarea}(T(r)\cap\{z:|z|>n\}) = O(e^{-cn}).$$

A result of Dyn′kin [17] then implies that, for any positive m,

$$\phi(z) = a_1 z + a_0 + a_{-1}z^{-1} + \ldots + a_{-m}z^{-m} + O(z^{-m-1}), \tag{8.4}$$

in $|z|>1$. This is helpful for deducing more delicate properties of f from g as we shall see in several examples later.

The following sections illustrate applications of Theorems 1.1 and 7.2. Some of these are new results, some are new proofs of known results and some show that certain known "pathological" examples can be taken in the Speiser class. For the most part, these sections are independent of each other and have been kept brief by leaving certain details to the reader. Perhaps the most interesting application is the existence of a function f in the Eremenko–Lyubich class with a wandering domain. This is placed near the end of the paper since the construction and proof is more complicated than the other applications. The wandering domain construction does not depend on the earlier examples, but understanding a few of the simpler cases might be a helpful "warm-up".

9. Application: countable singular sets

Recall that $\mathcal{B}$ denotes the transcendental functions with bounded singular set (critical values and finite asymptotic values) and $\mathcal{S}\subset\mathcal{B}$ are the functions with finite singular sets. Our first example is to show that any compact set can be the singular set of a function in $\mathcal{B}$. This is only meant to illustrate the method of applying our results; a theorem of Heins [32] says that any Suslin analytic set can be the set of finite asymptotic values.

COROLLARY 9.1. *Suppose that $E, F\subset\mathbb{C}$ are both bounded, countable sets and that E has at least two points. Then there is an $f\in\mathcal{B}$ such that E is the set of critical values and F is the set of finite asymptotic values.*

Proof. First assume that $\pm1\in E$ and the rest of $E\cup F$ is contained in $\frac{1}{2}\mathbb{D}$. The tree is shown in Figure 29. The shaded regions are D-components and L-components. Note that no two of these touch. All the other components are R-components. Add vertices

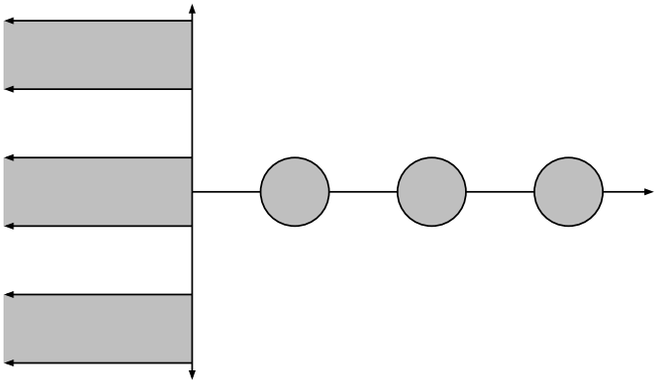

Figure 29. There is a critical point with prescribed critical value in each shaded disk, and a prescribed asymptotic value in each shaded half-strip. It is simple to place vertices on the tree that satisfy the necessary conditions.

along the positive real axis at the points where the circles cross the axis, and add vertices with approximately unit spacing along the rest of the boundary. For each disk we let $d{=}2$ and for the nth disk, choose the map ϱ as in the description of D-components to map 0 to the nth critical value. Choose τ for each L-component so that corners map to adjacent elements of $\mathcal{Z}$ (and hence the vertical side has τ image of length π) and add vertices to the horizontal edges by pulling back $\mathcal{Z}$ under τ (τ will essentially be the sinh function). Enumerate the shaded half-strips and choose ϱ for the nth half-strip to send 0 to the nth element of F. Choose τ for each R-component, so that the τ-image for every edge is $\geqslant\pi$. Then the conditions of Theorem 7.2 are satisfied and the desired map exists and has the specified singular values.

To deduce the general case, consider the holomorphic polynomial

$$p(z) = \tfrac{1}{2}z^3 - \tfrac{3}{2}z.$$

It is easy to check that ± 1 are the only critical points and the only critical values. Since p is cubic, every point except ± 1 has three distinct preimages. See Figure 30.

Note that 1 can be connected to ∞ by a preimage γ_+ of $(-\infty, -1]$ that lies in the upper half-plane. Similarly -1 can be connected to ∞ by a preimage γ_- of $[1, \infty)$. We can choose an open neighborhood U of $\gamma_+ \cup \gamma_-$ so that every point in the plane has at least one preimage that is not in U.

Now suppose E and F are as given in the lemma. By composing with a holomorphic linear map, we may assume, without loss of generality, that $\pm 1 \in E$. By our remarks above we can choose countable sets E' and F' so that $p(E'){=}E$ and $p(F'){=}F$ and a compact set K so that $E' \cup F' \subset K \subset \mathbb{C} \setminus U$. Since the complement of U is simply connected, we can choose a quasiconformal map ψ of the plane that fixes both -1 and 1 and so

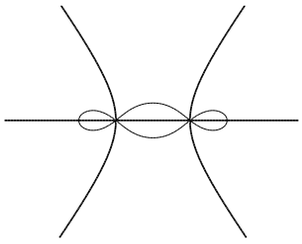

Figure 30. The thick curves form the preimage of the real axis under p and the thin curve is the preimage of the unit circle. The intersection points are ± 1. The unbounded arcs γ_+ and γ_- in the upper half-plane connect ± 1 to infinity and we can choose a neighborhood U of these two arcs so that every point has at least one preimage not in U.

that $\psi^{-1}(K) \subset D\left(0, \frac{1}{2}\right)$ (the quasiconstant will depend on the choice of K and U). Let $E'' = \psi^{-1}(E')$ and $F'' = \psi^{-1}(F')$. Then, by our earlier argument, there is an $f \in \mathcal{S}$ with critical values $E'' \cup \{-1, 1\}$ and finite asymptotic values F''. Thus $p \circ \psi \circ f$ is a quasiregular function with critical values E and asymptotic values F and hence by the measurable Riemann mapping theorem there is a quasiconformal ϕ so that $p \circ \psi \circ f \circ \phi$ is entire with the same singular set, proving the result. □

Since the singular set is the closure of the critical values and finite asymptotic values it is clear that we can achieve any compact set K as a singular set by applying the lemma to a countable dense subset of K.

10. Application: spiral tracts in $\mathcal{S}$

Consider Figure 31. The tree in this case is a spiral curve to ∞ so that widths of adjacent spirals are comparable and the vertices are spaced with gaps comparable to these widths. It is easy to see that T has bounded geometry and it is also easy to see that the τ-size of every edge is bounded below uniformly. In fact, it is obvious that (8.3) holds, so we can increase the number of vertices in the nth spiral by a factor of e^n and still maintain the hypotheses of Theorem 1.1 (this is because the hyperbolic distance in the tract from the origin to the nth spiral is greater than n, at least if the spirals are thin enough). Therefore not only does Theorem 1.1 apply, but ϕ is conformal off a set of finite area, because $T(r_0)$ has finite Lebesgue area. Thus Dyn′kin's estimate (8.4) holds for any m we want. It easy to see that we can make the tract spiral as quickly as we wish, and hence we have the following result.

COROLLARY 10.1. *For any function $\phi: [0, \infty) \to [0, \infty)$ that increases to ∞ there are an $f \in \mathcal{S}_{2,0}$, a $t_0 < \infty$ and a curve $\gamma: [0, \infty) \to \mathbb{C}$ along which f tends to infinity, such that,*

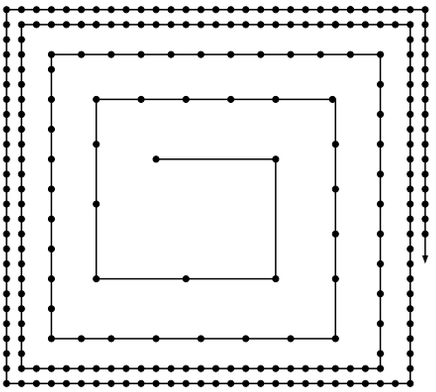

Figure 31. A spiraling tract with a single R-component.

for all $t>t_0$,

$$\arg(\gamma(t)) \geqslant \phi(|\gamma(t)|),$$

where arg *is a continuous branch of the argument on the simply connected domain*

$$\Omega = f^{-1}(\mathbb{C}\setminus[-1,1]).$$

This seems to be a new result even for $\mathcal{B}$, where the best previously result I know of gives a function with $\arg(\gamma(t))\geqslant C\log|\gamma(t)|$. See [27, Chapter VII].

11. Application: the area conjecture fails in $\mathcal{S}$

As noted earlier, the logarithmic area of a set E in the plane is defined as

$$\operatorname{logarea}(E) = \int_E \frac{dx\,dy}{x^2+y^2}.$$

The area conjecture asks if $\operatorname{logarea}(f^{-1}(K))<\infty$ whenever K is a compact set of $\mathbb{C}\setminus S(f)$ (recall that $S(f)$ are the singular values of f). A special case of this was asked by Eremenko and Lyubich in [22].

A counterexample to Epstein's order conjecture in $\mathcal{S}$ is given in [13], and this function is automatically a counterexample to the area conjecture as well, but an easier counterexample is illustrated in Figure 32.

The picture shows two versions of the tree; on the left is the tree itself with a single complementary component Ω, and on the right is the tree in cosh-coordinates with complement $\Omega'=\operatorname{arcosh}(\Omega)$. The second picture is easier to understand because of the exponential changes in scale in the first picture. In cosh-coordinates there is a central

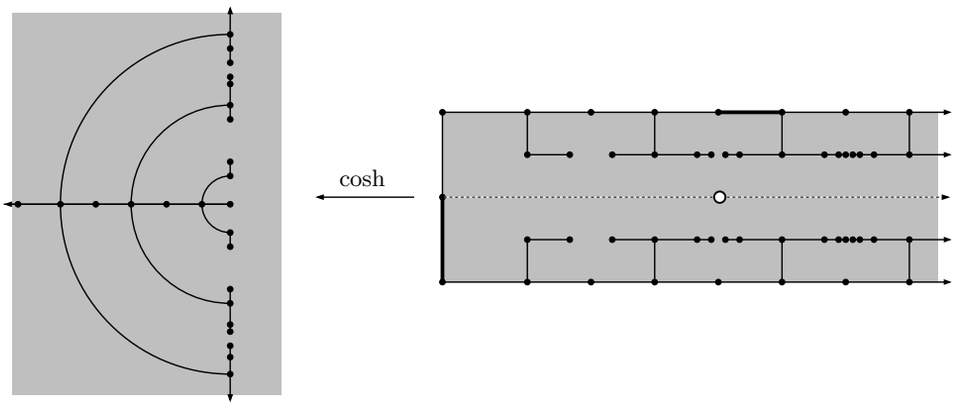

Figure 32. On the left is Ω, the tract of the area conjecture counterexample and on the right is $\Omega'=\operatorname{arcosh}(\Omega)$; the same example in cosh-coordinates. In the second picture, "rooms" are attached along a central strip by small gaps whose size is chosen so that edges on the top and bottom of the strip (thick edge) have approximately the same harmonic measure as the left side of the strip (thick edge) when viewed from a point (white dot) on the axis of the domain (dashed line).

strip along which are attached "rooms" and the size of the opening leading to each room is chosen so that

$$\varrho(\gamma_j, x_j) = \varrho(x_j, x_0) + O(1), \tag{11.1}$$

i.e., we have equality up to a bounded additive factor in (8.1). The gaps can easily be chosen with the desired property by a continuity argument that decreases the each gap until the desired equality holds, plus an argument that shows that changes to other gaps does not effect the hyperbolic distance associated with any particular gap by more than $O(1)$. Vertices must be added with geometric decaying spacing near the endpoints of each gap to give the bounded-geometry property.

With these choices, τ will have bounded derivative near the middle of each room and along the top edge. This implies that $\{z:|g(z)|<R\}$ will contain a disk of radius comparable to 1 in each "room" and the union of these disks has infinite logarithmic area. The quasiconformal change of variable ϕ preserves the strip in cosh-coordinates and maps these disks to regions of Euclidean comparable area, so the entire function $f=g\circ\phi^{-1}$ disproves the area conjecture.

12. Application: a stronger counterexample to the area conjecture

We just constructed an entire function so that $\{z:|f(z)|<R\}$ always has infinite logarithmic area. We can strengthen this to a function so that $\{z:|f(z)|>\varepsilon\}$ always has finite Lebesgue area. There are several ways to do this with three singular points; I will give an

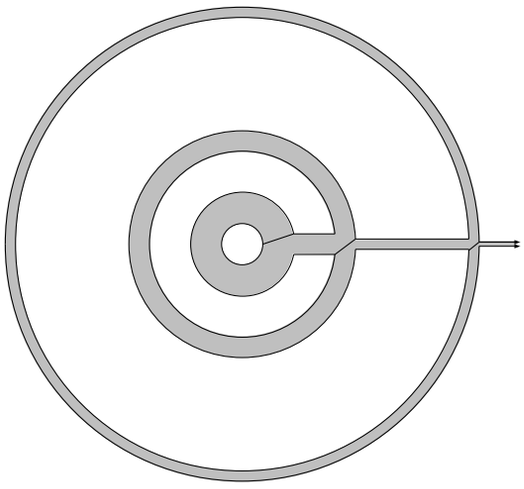

Figure 33. The tract for an $\mathcal{S}_3$ function so that $\{z:|f(z)|>R\}$ has finite Lebesgue area for any $R>0$. There are infinitely many bounded components, but only one unbounded component (the shaded region). The difficulty is to add vertices that give bounded geometry and satisfy Theorem 7.2.

example using high-degree critical points, but it is also possible using two critical values and one finite asymptotic value (I leave this as an exercise for the reader). I do not know if such an example is possible with only two finite singular values.

COROLLARY 12.1. *There is a function $f\in\mathcal{S}_3$ with critical values $\{-1,0,1\}$ and no finite asymptotic values so that* $\operatorname{area}(\{z:|f(z)|>\varepsilon\})<\infty$ *for every $\varepsilon>0$.*

Proof. The tract for this example is Figure 33. There are countably many bounded components

$$\Omega_j=\{z:e^j+\varepsilon_j<|z|<e^{j+1} \text{ and } \operatorname{dist}(z,\mathbb{R}^+)>\varepsilon_j\},$$

that approximate a slit annulus and a single unbounded component Ω that surrounds each of these bounded components (Ω is the shaded region in Figure 33). Assume $\varepsilon_j=e^{-2j}$.

We can think of Ω as a series of alternating annuli and rectangles joined end-to-end. Fix a base point x_0 and let γ be the axis of Ω with base x_0. Let γ_n the part of γ between its first crossing of $\{z:|z|=e^j\}$ and its first crossing of $\{z:|z|=e^{j+1}\}$. The hyperbolic length of γ_j is $\geqslant e^j/\varepsilon_j\geqslant e^{3j}$. Therefore the spacing of the $V=\tau^{-1}(Z)$ along $\partial\Omega_j$ is $O(e^{-e^{3j}})$. Choose any basepoint for Ω_j that is about distance e^j from the boundary, and let ω denote harmonic measure with respect to this point. The Euclidean length of an arc I on $\partial\Omega_j$ satisfies

$$\frac{1}{C}\ell(I)^2e^{-2j}\leqslant\omega(I)\leqslant C\ell(I)e^{-j}.$$

This is because if we normalized to unit size, harmonic measure of the sides would be comparable to arclength measure, except near the corners where harmonic measure

is comparable to $|z-c|\,ds$, where c is the corner (this can be seen by using $\sqrt{z-c}$ to "open" the corner to a C^1 curve and using conformal invariance of harmonic measure). Combined with our earlier remarks, we see that if we divide $\partial\Omega_j$ into about e^{6j} arcs of equal harmonic measure, these arcs will each have Euclidean length between e^{-2j}/C and Ce^{-5j}. By our earlier remarks, these will contain many integer points for the unbounded component and hence Theorem 1.1 applies. □

Hayman and Erdős [30] asked about the smallest possible growth rate for a function f with $\operatorname{area}(\{z:|f(z)|>R\})<\infty$, and this was answered by Gol′dberg [26] and Cámera [15] who showed that for such an f,

$$\int^{\infty} \frac{r\,dr}{\log\log M(r,f)} < \infty,$$

where $M(r,f)=\sup_{|z|=r}|f(z)|$. Conversely, for any φ such that

$$\int^{\infty} \frac{r\,dr}{\varphi(r)} < \infty, \tag{12.1}$$

there is an entire function f with finite-area level set and such that $\log\log M(r,f)=O(\varphi(r))$ for large enough r. By taking $\varepsilon_k=e^k/\varphi(e^k)$ our example shows that this f can be taken in $\mathcal{S}$, at least if we also assume the regularity condition

$$\sum_{j<k} \varphi(2^j) = O(\varphi(2^k))$$

(however, since (12.1) implies φ grows at least like r^2, this is not too restrictive).

13. Application: Wiman's minimum modulus conjecture in $\mathcal{S}$

Another result where we can show that extreme behavior among entire functions is attained in $\mathcal{S}$ concerns Wiman's problem on minimum modulus. For an entire function f, we let

$$m(r)=\min_{|z|=r}|f(z)| \quad \text{and} \quad M(r)=\max_{|z|=r}|f(z)|.$$

By definition $m(r)\leqslant M(r)$, but it is interesting to ask how much smaller can m be compared to M? Obviously we have to avoid zero's of f, but it is reasonable to ask if there is a finite α so that for any entire function, $m(r)\geqslant M(r)^{-\alpha}$ along some sequence of radii tending to infinity? The function e^z shows that we cannot take $\alpha<1$. Wiman proved in [48] that, for any ε and any non-vanishing entire function f,

$$m(r) > M(r)^{-1-\varepsilon}$$

for some sequence of r's tending to ∞. He conjectured this was true in general and this was verified by Beurling [8] in the special case $|f(r)|=m(r)$ (i.e., the minimal values are attained along $\mathbb{R}^+$), but was disproved by Hayman in general [29]. We can show that a Hayman-type counterexample can be taken in $\mathcal{S}_3$.

COROLLARY 13.1. *There are $A>0$, $r_0<\infty$ and an entire function $f\in\mathcal{S}_{3,0}$ such that*

$$m(r) < M(r)^{-A\log\log\log M(r)} \tag{13.1}$$

for all $r>r_0$. Hence $m(r)<M(r)^{-C}$ for every C and r large enough.

Proof. The tract is shown in Figure 34. In this case there are infinitely many bounded components, all disks of radius 1, with centers distributed along a spiral curve of the form

$$t \longmapsto (3+2t)\exp(2\pi i t), \quad t \geqslant 0.$$

The single unbounded tract is bounded by the curve γ_1,

$$t \longmapsto (2+2t)\exp(2\pi i t), \quad t \geqslant 0,$$

the bounded components and radial segments joining the bounded components to γ_1, as in Figure 34.

Let 0 be the base point of Ω. A bounded component Ω_j in the nth spiral (corresponding to a value of $t=n+O(1)$) has hyperbolic distance $\geqslant Cn^2$ from 0 (the kth spiral has length $\simeq k$ and $\sum_{k=1}^{n} k\simeq n^2$). Therefore $V=\tau^{-1}(Z)$ will have about $\exp(Cn^2)$ points on the boundary of Ω_j and the separation between them is $O(\exp(-Cn^2))$. Therefore we can apply Theorem 7.2 with a critical point of order $\varepsilon\exp(C_1n^2)$.

Any large circle centered at the origin of radius $r\geqslant n$ will pass within $O(1/n)$ of one of the bounded components in at least the $\frac{1}{2}n$th spiral. Thus there is a point on this circle where our quasiregular function g is less than

$$\left(\frac{C_2}{n}\right)^{\exp(C_1n^2)} = \exp((\log C_2-\log n)\exp(C_1n^2)) = O(\exp(C_3\exp(C_1n^2))^{-(\log n)/2}),$$

for large n. On the other hand, $|\tau|=O(\exp(C_3n^2))$ at every point on the circle, so

$$M(r) \leqslant 2\exp(C_4\exp(C_5n^2)).$$

Thus

$$\log\log\log M(r) \leqslant C_6\log n,$$

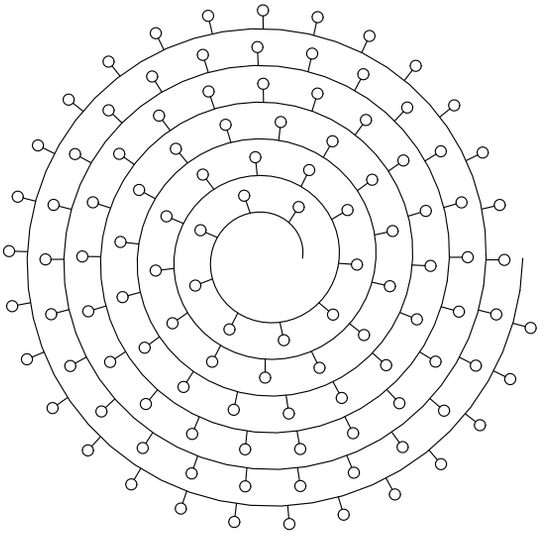

Figure 34. The tract for an $\mathcal{S}_3$ function disproving Wiman's conjecture. Like Hayman's example, high-degree critical points are distributed along a spiral so any circle centered at the origin comes close to the center of one of the bounded components. Some estimate of the hyperbolic metric in the unbounded tract is needed to verify that Theorem 7.2 can be applied.

so

$$\begin{aligned} m(r) &\leqslant C\exp(C_3\exp(C_1n^2))^{-(\log n)/2} \\ &\leqslant C\exp(C_4\exp(C_3n^2))^{-(C_1/C_3)(C_3/C_4)(1/2)\log\log\log M(r)} \leqslant CM(r)^{-A\log\log\log M(r)}. \end{aligned}$$

This is the correct estimate, but is valid for the quasiregular function g, not the entire function $f=g\circ\phi^{-1}$. However, ϕ is conformal except on $T(r_0)$ and this set has area $O(e^{-Cn^2})$ in the nth spiral, so Dyn′kin's estimate implies ϕ is conformal near ∞ with an error of size $O(|z|^{-m})$ for any $m>0$ that we want. Taking $m=1$ says that ϕ maps a circle of radius n around the origin into an annulus of width $O(1/n)$ and hence the image curve will still pass within distance $O(1/n)$ of the center of the same bounded component. Thus the estimates above also apply to f. □

14. Application: folded functions on the disk

As noted in the introduction, the proof of Theorem 1.1 applies to domains other than the plane. If we cut the unit disk into simply connected pieces and τ conformally maps the components of $\Omega=\mathbb{D}\setminus T$ to $\mathbb{H}_r$ so that the induced partitions of $\partial\mathbb{H}_r$ satisfy the conditions of Theorem 1.1, then we get a quasiregular function g on all of $\mathbb{D}$ that extends the

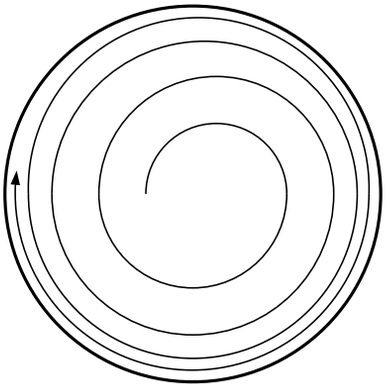

Figure 35. A curve spiraling out the boundary of the disk; this curve gives the tree we use to prove Corollary 14.1.

restriction of $\cosh\circ\tau$ to $\mathbb{D}\setminus T(r_0)$. The quasiconformal correction map ϕ can be chosen to map $\mathbb{D}\to\mathbb{D}$, so we end up with a holomorphic function f on $\mathbb{D}$ that approximates $\cosh\circ\,\tau$. Adapting one of our previous examples from the plane to the disk gives the following result.

COROLLARY 14.1. *There is a holomorphic function on the disk with only two critical values so that* $\{z:|f(z)|>2\}$ *spirals out to* $\partial\mathbb{D}$ *as quickly as we wish.*

See [25] for a discussion of such functions, first constructed by Valiron. This function is strongly non-normal in the sense of [40] and is both a finite-type map in the sense of Epstein and an Ahlfors islands map. See [18]. Other examples constructed for the plane can also be adapted to the disk, e.g., using the idea in §12 we can build a function f on $\mathbb{D}$ with three critical points so that $\{z:|f(z)|>\varepsilon\}$ has finite hyperbolic area for every $\varepsilon>0$.

15. Application: Belyi functions on the plane

Suppose T is a finite bounded-geometry tree. Then $\Omega=\mathbb{C}\setminus T$ is unbounded and connected, but not simply connected. There is a covering map $\sigma:\mathbb{H}_r\to\Omega$. By rescaling, we may assume that every side of T (there are only finitely many) corresponds to an interval of length $\geqslant\pi$ in a periodic partition of $\partial\mathbb{H}_r$. We can define a corresponding periodic folding map and deduce that there is a quasiconformal covering map $\psi:\mathbb{H}_r\to\Omega$ so that $g=\cosh\circ\,\sigma^{-1}$ is well defined and quasiregular. Then the measurable Riemann mapping theorem gives a quasiconformal map ϕ of the plane so that $f=g\circ\phi^{-1}$ is entire and is a finite covering from $\phi(\Omega)$ to $U=\mathbb{C}\setminus[-1,1]$. This means that f is a polynomial with critical values ±1. Moreover, ϕ's dilatation is supported in $T(r_0)$; if this has small area,

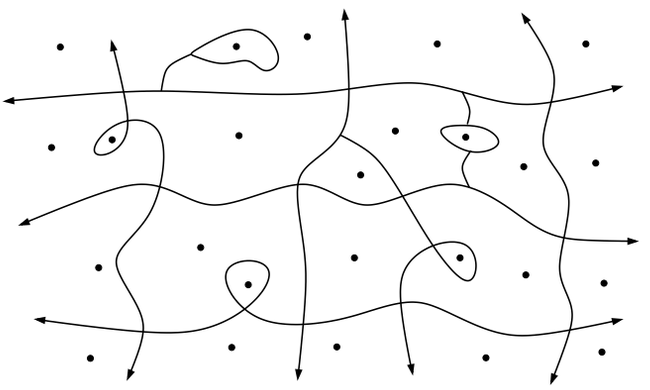

Figure 36. For any bounded-geometry partition of the plane into finite-sided regions, there is a Belyi function (with critical points ± 1 and ∞) so that $f^{-1}([-1,1])$ approximates the boundary of the partition and $f^{-1}(\infty)$ approximates any choice of one point per region.

then $\phi(T)$ approximates T in the Hausdorff metric. This shows that the results of this paper provide an alternative approach to the main result of [10]. The same argument works on a bounded domain where the boundary is partitioned into a finite number of arcs with bounded-geometry and we choose one interior point to be mapped to ∞.

If Γ is a bounded-geometry graph that partitions the plane into finite-sided regions, then for each region we can define a periodic covering map as above that satisfies the τ-length $\geqslant \pi$ condition, and apply quasiconformal folding to make opposite sides of every edge match. Thus for any bounded-geometry partition of the plane $\mathbb{C}\backslash\Gamma = \bigcup_n W_n$ and any choice of a point $z_n \in W_n$ near the center of W_n, there is a meromorphic function f that has exactly the three critical values $\pm 1, \infty$, and so that $f^{-1}([-1,1])$ approximates Γ in the Hausdorff metric and $f^{-1}(\infty)$ approximates $Z = \bigcup_n \{z_n\}$ in the Hausdorff metric. See Figure 36.

On a compact Riemann surface, a meromorphic function with exactly three critical values is called a Belyi function. Not every compact surface X supports such a function (Belyi's theorem [4] classifies such surfaces as a certain countable family of algebraic varieties, so only countably many compact surfaces have a Belyi function), but our methods show that such surfaces are dense in each Teichmüller space and $f^{-1}([-1,1])$ can be taken to approximate (in an appropriate sense) any compact connected set whose complementary components are simply connected. Belyi functions on non-compact surfaces have been considered by Eremenko and Langley, e.g., [20], [33] and [36].

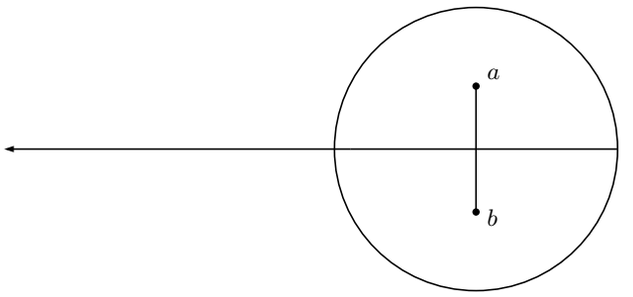

Figure 37. This tree cuts $W=\mathbb{C}\setminus\{a,b\}$ into three simply connected regions. To make the τ-sizes $\geqslant\pi$, the spacing between vertices will have to be larger than $|z|$ near ∞, and larger than $|z-a|^{-3}$ near the punctures.

16. Application: folding a pair of pants

Epstein [18] defines a finite-type map f as a holomorphic function defined on an open subset W of one compact Riemann surface Y and taking values in another compact Riemann surface X, such that

(1) the set S of singular values is finite;
(2) no puncture of W is a removable singularity of f;
(3) f is non-constant on every component of W.

The first condition means that there is a finite set $S\subset X$ such that the map, when restricted to the preimage of $X\setminus S$, is a covering map onto $X\setminus S$. Examples of finite-type maps include rational maps and Speiser class transcendental entire functions, and the definition of finite type allows various results of the dynamics of such maps to be generalized to other settings.

The methods of this paper can be used to construct examples in a more general setting. For example, Figure 37 shows a graph $T\subset W=\mathbb{C}\setminus\{a,b\}$ so that $W\setminus T$ consists of three simply connected domains. Choose τ to be conformal on each component and mapping a, b and ∞ to ∞. It is easy to check that we can choose vertices for T and the map τ so that the τ-size of every edge is $\geqslant\pi$ and adjacent edges have images of comparable lengths. Thus taking each component to be an R-component and applying the folding construction gives a quasiregular g on W and a holomorphic $f=g\circ\phi^{-1}$ on $\phi(W)$ (since any two thrice-punctured spheres are conformally equivalent, we may assume $\phi(W)=W$). Thus f has only two singular values (the critical values ±1) and has essential singularities at $\{a,b,\infty\}$. Hence f is a finite-type map from the thrice-punctured sphere to the plane.

It is particularly interesting to construct finite-type maps where the target X is a compact, hyperbolic Riemann surface and $W\subset Y=X$; in this case the map can be iterated. For example, if W is a disk in Y, just map W conformally to the unit disk

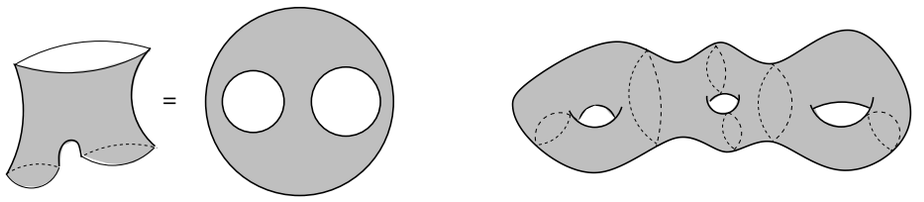

Figure 38. A pair of pants is a planar domain; every compact, hyperbolic surface can be decomposed into pieces like this bounded by closed geodesics.

and then follow by the universal covering map to X. As far as I know, all previously known examples of finite-type maps into hyperbolic targets are of this form or closely related. However, we can construct examples where W has more interesting topology using quasiconformal folding.

A Riemann surface is called a "pair-of-pants" if it is conformally equivalent to a planar domain with three boundary components. Using Koebe's theorem for finitely connected domains, we may take the boundaries to be circles or points. We say the pair-of-pants is *non-degenerate* if none of the boundary components are points. Every compact, hyperbolic Riemann surface has a decomposition into such pieces (hyperbolic means the universal cover is the disk). See Figure 38.

Let f be the finite-type map on $W=\mathbb{C}\setminus\{a,b\}$ constructed above and let

$$W'=\{z:|f(z)|<R\}.$$

Then W' is an open planar domain with three complementary components and hence is conformally equivalent to some pair-of-pants Y. See Figure 39. Moreover, $h=f/R$ maps W' onto the unit disk and is a covering on $\mathbb{D}\setminus\{\pm 1/R\}$. If we precede h by the conformal map $Y\to W'$ and follow it by the universal covering map to any hyperbolic Riemann surface X, we get a finite-type map F from Y to X. If X is first type (i.e., the limit set of the covering group is the entire circle) then F has an essential singularity at every point of ∂Y. This happens if X is compact and hyperbolic. If we choose X so that it contains Y (e.g., if X is two copies of Y glued along the boundaries), then we have a finite-type map from a topologically non-trivial open subset of X to all of X. This is our "interesting" finite-type map.

The proof above builds a pair-or-pants that supports a finite-type map (with just two critical values) into any compact hyperbolic surface. By changing the value of R we obtain another pair-of-pants that is clearly conformally distinct, so we actually have produced a continuous 1-parameter family of such surfaces. We can also produce different examples by altering the choice of τ on each component independently, or by choosing the shape of the initial tree T differently, or by allowing more than two critical values and

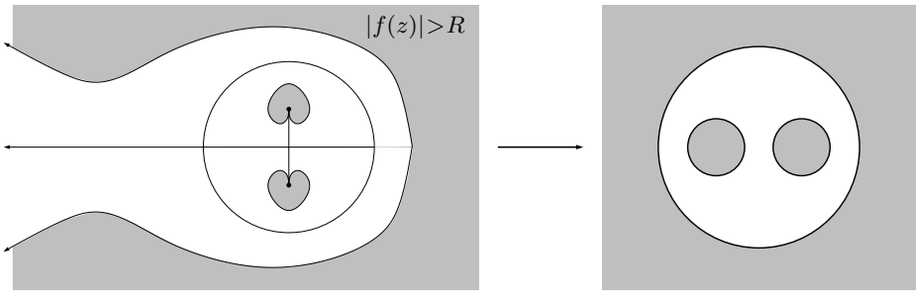

Figure 39. The set $\{z:|f(z)|\geqslant R\}$ has three components at positive distance from each other. The complement of the closure is an open set with three boundary components and hence is conformally equivalent to some pair-of-pants.

taking functions quasiconformally equivalent to f. Given this freedom, it seems reasonable, but not obvious, that all non-degenerate pairs-of-pants have finite-type maps into any compact, hyperbolic Riemann surface (but perhaps the example of Belyi functions existing only on countably many compact Riemann surfaces should make us cautious).

Next, we will produce a compact surface X of genus $g\geqslant 2$, a closed disk $D\subset X$ and a finite-type map $X\setminus D\to X$. Start with a compact, hyperbolic surface X' and form a simply connected subregion $U\subset X'$ by removing closed geodesics from X. Choose a point $a\in U$ and a curve γ that connects ∂U to a so that $\partial U\cup\gamma$ can be made into a bounded-geometry tree with τ-sizes $\geqslant\pi$. See Figure 40. As before, we get a holomorphic function f on a quasiconformally equivalent surface X'' that has two critical values and an essential singularity at a. Restricting f/R to $W=\{z:|f(z)|<R\}$ gives a map to the disk that we can follow by the covering map to X'. He and Schramm's countable version of Koebe's theorem [31] implies the set W is conformally equivalent to $X\setminus D$ for some compact X and a closed disk $D\subset X$. Thus mapping $X\setminus D\to W\to\mathbb{D}\to X$, by the maps described above gives a finite-type map. The argument can be extended to give examples with any number of disjoint disks removed. As with pairs-of-pants, this argument only produces examples of such surfaces and it is not yet clear whether finite-type maps will exist for every surface of this type.

17. Application: a wandering domain in $\mathcal{B}$

The Fatou set $\mathcal{F}(f)$ of an entire function f is the union of disks on which the iterates of f form a normal family. The Julia set $\mathcal{J}(f)$ is the complement of the Fatou set and is always non-empty, closed and uncountable (see e.g., the surveys [5] and [42]).

A wandering domain is a connected component of $\mathcal{F}(f)$ whose images under iterates of f are all disjoint. Adapting the argument of Sullivan [46] for the rational case,

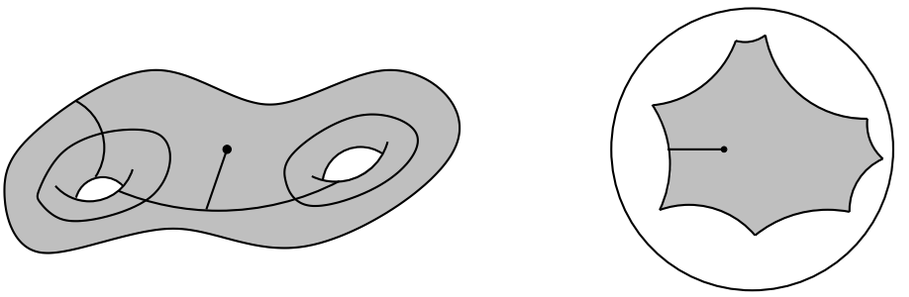

Figure 40. Building a finite-type map from $X \setminus D$ to X. The picture is clearer for the associated fundamental domain in $\mathbb{D}$.

Eremenko and Lyubich proved in [22] and Goldberg and Keen proved in [28] that the Fatou set of a function in the Speiser class $\mathcal{S}$ cannot have a wandering domain. However, the question of whether this is possible for a function in $\mathcal{B}$ has remained open. We will use Theorem 7.2 to prove the following result.

THEOREM 17.1. *There is an $f \in \mathcal{B}$ whose Fatou set contains a wandering domain.*

Eremenko and Lyubich proved that if Ω is a wandering domain for $f \in \mathcal{B}$, then the iterates of f on Ω cannot tend to ∞. In our example, the orbits are unbounded, but return to a compact set infinitely often, as required by their result. The only previous example of a wandering domain that does not iterate to ∞ was given by Eremenko and Lyubich in [21]. It is currently an open question whether any entire function can have a wandering domain with a bounded orbit. By a result of Bergweiler, Haruta, Kreite, Meier and Terglane [7], every limit point of the orbit of a wandering domain must be a limit point of the post-singular set $P(f)$ (the union of iterates of the singular set). In our case, the only limit points of $P(f)$ are the iterates of $\pm\frac{1}{2}$ which form real sequences tending to ∞. Our function is bounded on a curve tending to infinity, so all the components of the Fatou set are simply connected by [21, Lemma 4] (this is true for any function in $\mathcal{B}$).

Rempe-Gillen and Milhaljević-Brandt have shown that a real function in $\mathcal{B}$ has no wandering domains if the iterates of the singular set satisfy certain conditions [38]. In [23], Fagella, Godillon and Jarque have used the methods in [38] to show that the function built here has no other wandering domains than the "obvious" ones that are forced by the construction. Their proof modifies the proof of Theorem 17.1 and verifies certain details of the proof that are left to the reader here. They use their modified construction to build two functions $f, g \in \mathcal{B}$ so that neither f nor g has a wandering domain, but both $f \circ g$ and $g \circ f$ do have wandering domains.

Theorem 17.1 follows from the following result.

LEMMA 17.2. *There is an $f\in\mathcal{B}$, a disk D_0 and an increasing sequence of integers $\{n_k\}_{k=1}^{\infty}\nearrow\infty$ such that, if we set $D_n=f(D_{n-1})$ for $n\geqslant 1$, then*

(1) *the diameter of D_n tends to zero*;

(2) $\operatorname{dist}(0,D_{n_k})\nearrow\infty$, *but* $\operatorname{dist}(0,D_{n_k+1})\leqslant 1$ *for all* $k=1,2,\ldots$.

It is fairly easy to see that the two properties in the lemma imply that the Fatou set of f has a wandering domain. First, the iterates of f are clearly normal on D_0 since (1) implies that every subsequence has a further subsequence that either approaches ∞ uniformly on D_0 or converges to a finite constant. Thus D_0 and all its images are in the Fatou set. However, we claim they must all be in different components. Suppose $n<m$ and D_n and D_m were in the same component Ω of $\mathcal{F}(f)$. Since f is a holomorphic map from Ω to $f(\Omega)$, the hyperbolic distance between D_m and D_n cannot increase under iteration. If $n_k>m$ and we iterate n_k+1-m times then D_m maps to D_{n_k+1} near the origin, but D_n maps to $D_{n_k+1-m+n}$ whose distance from 0 grows to ∞ with k for fixed n and m (because its $(m-n)$-th iterate D_{n_k} tends to ∞ with k). The Julia set of f contains at least two points (in fact, a continuum of points by a result of Baker in [2]) and the Fatou component containing the (n_k+1-m)-th iterates of D_m and D_n is in the complement of the Julia set. Thus the hyperbolic distance between the iterates of D_n and D_m in any Fatou component is bounded below by the hyperbolic distance in the complement of the Julia set, and this clearly increases to ∞ with k. This contradicts the Schwarz lemma, i.e., the fact that the hyperbolic distance between the iterates of D_n and D_m must stay bounded. Thus every disk D_n is contained in a different component of the Fatou set and these components form the orbit of a wandering domain.

We will first sketch the proof of Lemma 17.2 and then give the details. Our entire function will map $\mathbb{R}$ to $\mathbb{R}$ and the point $x_0=\frac{1}{2}$ will iterate to ∞. We will choose a tiny disk D_0 in the upper half-plane, just above $\frac{1}{2}$, and the orbit of D_0 will follow the orbit of $\frac{1}{2}$ for several iterations, but the two orbits eventually diverge; the orbit of $\frac{1}{2}$ remaining on the real line and the orbit of D_0 moving away from the real line and landing near a high-degree critical point.

The critical point compresses the image of D_0 (which has greatly expanded while following the orbit of $\frac{1}{2}$) and maps it very close to its critical value, which we will chose to be very near $\frac{1}{2}$. The process now repeats: the image follows the orbit of $\frac{1}{2}$ again until it diverges and lands near a different critical point, which compresses the image again and returns it to another starting point near $\frac{1}{2}$. The starting points are closer to $\frac{1}{2}$ each time we return near the origin, and this allows the next expansive stage to follow the orbit of $\frac{1}{2}$ longer than the previous time. Thus the orbit of D_0 is unbounded, but does not converge to ∞ (this oscillation is required by the result of Eremenko and Lyubich). The degrees of the critical points are chosen so the compression near them is greater

than the expansion at earlier times, so the diameters of the iterates tend to zero (but not monotonically). The critical values of our example will be $\{\pm\frac{1}{2}, \pm 1\}$ plus sequences that converge to $\pm\frac{1}{2}$ (we can even say they converge within vertical cones at these points and we can make the rate of convergence as fast as we wish, but I do not know any application for this extra information).

Proof of Lemma 17.2. We start by describing a function f obtained by QC folding that has only finitely many critical values and then we will describe how to make a sequence of small perturbations to this function that create new critical values. The limit of these perturbations will be the desired function with bounded singular set and a wandering Fatou component.

We will build our function with Theorem 7.2, using only R-components and D-components. These are arranged as in Figure 41. The arrangement is symmetric with respect to both the real and imaginary axes, so our functions will satisfy

$$f(\bar{z}) = \overline{f(z)} \quad \text{and} \quad f(-z) = f(z).$$

We will specify the construction in the first quadrant, the rest being filled in by symmetry.

There is a horizontal half-strip

$$S_+ = \{x+iy : x > 0 \text{ and } |y| < \tfrac{1}{2}\pi\}$$

that is conformally mapped to $\mathbb{H}_r$ by $\lambda \sinh$, where the positive integer λ will be chosen below to make sure $\frac{1}{2}$ iterates to ∞.

We also place disks

$$D_k = D(z_k, 1) = D(\pi k + i\pi, 1)$$

in the region above S_+. These are mapped to the unit disk by the maps $\sigma((z-z_k)^{d_k})$, where σ is a quasiconformal transformation of the disk sending 0 to $\frac{1}{2}$ that is conformal on $\frac{3}{4}\mathbb{D}$ and $\{d_k\}_{k=1}^{\infty}$ is a sequence of integers tending quickly to infinity (below we will specify two conditions that this sequence must satisfy). Our function f will have critical points of degree d_k in the disks D_k, with critical values $\pm\frac{1}{2}$. Such a function cannot have a wandering domain since it is the Speiser class, but our construction will perturb infinitely many of the critical values to form a sequence converging to $\frac{1}{2}$. The perturbed function has an infinite, but bounded, set of critical values and will also have a wandering Fatou component.

We then connect each disk D_k to ∂S_+ by a subsegment of $\{z{:}\mathrm{Re}(z){=}\mathrm{Re}(z_k)\}$ and connect it to ∞ by a vertical ray on the same line. This produces vertical regions that are almost half-strips, except for the indentations caused by the disks. See Figure 41. We will let S_k denote the region that is between D_k and D_{k+1}. This region is mapped

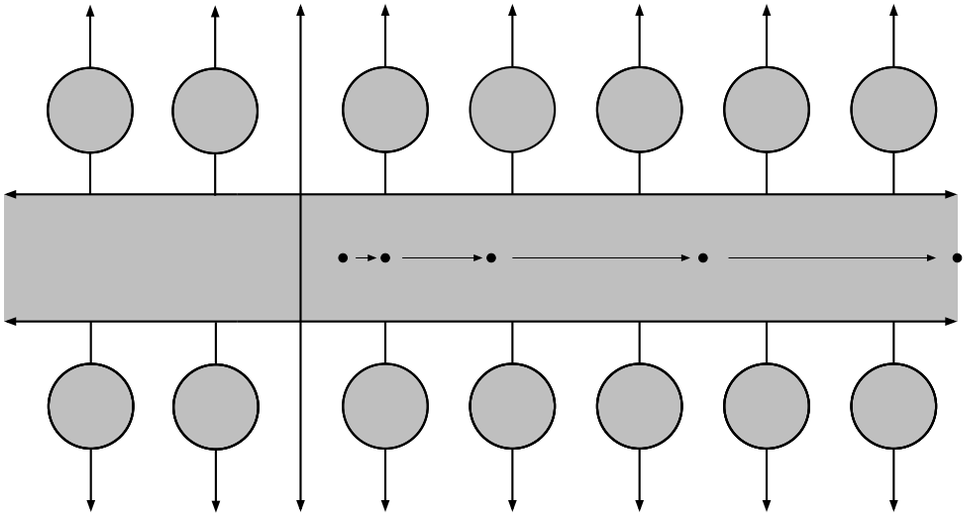

Figure 41. The tracts for our wandering domain example. The points and arrows show the orbit of $\frac{1}{2}$. The wandering domain follows this orbit for a while but eventually lands in one of the shaded disks, where it is mapped back to a neighborhood of $\frac{1}{2}$ and starts to follow the orbit of $\frac{1}{2}$ again.

to $\mathbb{H}_r$ by a conformal map that we choose so that the corresponding partition of ∂S_k is finer than the partitions induced by S_+ or ∂D_k and ∂D_{k+1} on the common boundary arcs. This means that Theorem 7.2 can be applied and that all the folding takes place in the S_k (so no folding occurs in S_+ or D_k).

Suppose that $\{d_k\}_{k=1}^{\infty}$ is already fixed and ϕ is the quasiconformal map given by Theorem 7.2 so that $f = g \circ \phi$ is entire, where g is the quasiregular function defined in the theorem. The formula for g in these regions is given by

$$g(z) = \cosh(\lambda \sinh(z)) \quad \text{on } S_+ \setminus T(r),$$

and

$$g(z) = \sigma((z - z_k)^{d_k}) \quad \text{on each } D_k \setminus T(r).$$

Restricting the foldings to the regions $\{S_k\}_{k=1}^{\infty}$, also means that ϕ is conformal on S_+ and each D_k. The dilatation of ϕ is supported inside $T(r_0)$, and this neighborhood of T decays exponentially in $|z|$. In particular, Dyn′kin's theorem implies that we may normalize ϕ so that it fixes 0, maps $\mathbb{R}$ one-to-one to itself and satisfies

$$\phi(z) = z + \frac{a_1}{z} + O(|z|^{-2})$$

near ∞. Since ϕ is conformal on a strip of width π centered along $\mathbb{R}$, we can deduce that the image of this strip contains and is contained in strips of comparable widths and

that ϕ' is bounded and bounded away from zero on $\mathbb{R}$. Moreover, these bounds do not depend on λ (in fact, as λ increases, the neighborhood $T(r_0)$ decreases and ϕ converges to the identity, so the bounds actually improve as λ grows).

Thus using the chain rule and the fact that $\sinh(x)>x$ for $x>0$, we get

$$\begin{aligned} f'(x) &= \frac{d}{dx}\cosh(\lambda\sinh(\phi(x))) \\ &= \sinh(\lambda\sinh(\phi(x)))\lambda\cosh(\phi(x))\phi'(x) \geqslant \lambda^2\phi^2(x)\phi'(x) \geqslant 16x, \end{aligned}$$

if we choose λ so that $\phi' \geqslant 4/\lambda$. Integrating implies $f(x)>8x^2$, which certainly implies that $\frac{1}{2}$ will iterate to ∞ under f (obviously a much better estimate is valid away from 0 and $\frac{1}{2}$ iterates to ∞ much faster than this estimate indicates).

Let $x_0=\frac{1}{2}$ and define a sequence by $x_n=f(x_{n-1})$. By our previous remarks this is an increasing sequence that converges to infinity. For each n choose an integer p_n so that $|\pi p_n - x_n|$ is minimized. Let $\widetilde{D}_n=D_{p_n}$ and let $\tilde{z}_n=z_{p_n}$ be its center. Then $|x_n-\mathrm{Re}(\tilde{z}_n)|\leqslant\frac{1}{2}\pi$ and hence $\widetilde{D}_n\subset V_n=D(x_n,5)$.

Let f^j denote the jth iterate of f and consider the preimage of V_n under f^n. This map has a univalent branch on V_n that maps V_n to a neighborhood W_n of $\frac{1}{2}$, and by the usual distortion theorems, $\frac{1}{4}D_n\subset V_n$ (concentric disk, one quarter the radius) is mapped to a region in the upper half-plane of comparable size and whose shape is a uniformly bounded distortion of a disk. Thus the preimage of $\frac{1}{4}\widetilde{D}_n$ contains a disk U_n of comparable size centered at the preimage of $\tilde{z}_n$. U_n has diameter comparable to

$$r_n = \left(\frac{d}{dx}f^n\left(\frac{1}{2}\right)\right)^{-1}.$$

What happens to U_n under iteration by f? It follows the iterates of $\frac{1}{2}$, but on the nth iteration it leaves the strip S_+ and enters the disk $\frac{1}{4}\widetilde{D}_n$. If we iterate f one more time then the image of U_n lands in the f-image of $\frac{1}{2}\widetilde{D}_n$. In $\widetilde{D}_n$ the map f is ϕ composed with

$$(z-\tilde{z}_n)^{d_{p_n}},$$

which is then composed with ϱ. Our estimates on ϕ imply that it maps $\frac{1}{4}\widetilde{D}_n$ into $\frac{1}{2}\widetilde{D}_n$ when n is large enough. The power term maps $\frac{1}{2}\widetilde{D}_n$ to a disk of radius

$$\left(\tfrac{1}{2}\right)^{d_{p_n}}$$

centered at the origin, and then ϱ moves this disk to contain the point $\frac{1}{2}$. We choose d_{p_n} to be so large that the radius of this disk is much less than r_{n+1}, i.e.,

$$d_{p_n} \gg \log_2 \frac{1}{r_{n+1}}.$$

This is the first of the two conditions that determine our choice of $\{d_k\}_{k=1}^{\infty}$.

The condition on $\{d_k\}_{k=1}^{\infty}$ might appear circular, since it depends on r_n, which depends on f, which depends on ϕ, which depends on a choice of $\{d_k\}_{k=1}^{\infty}$. However, as elements of $\{d_k\}_{k=1}^{\infty}$ increase, Theorem 7.2 implies the dilatation of ϕ remains uniformly bounded and is supported on smaller neighborhoods of T, so one can extract a subsequence that converges uniformly on compact subsets. This means that the corresponding entire functions f also converge uniformly on compact subsets of S_+ which implies the r_n's converge to non-zero limits. Thus each r_n has a positive lower bound, independent of how we choose the d_k's, and if we use these lower bounds to choose d_{p_n}, we get the desired inequalities.

So the $(n+1)$-st iterate of U_n is back near $\frac{1}{2}$ and is much smaller than U_{n+1}, but is not inside U_{n+1}. If we can get $f^{n+1}(U_n) \subset U_{n+1}$ then our induction will be complete and we will have a disk with an unbounded orbit that keeps returning to $\mathbb{D}$.

To get U_n to return inside U_{n+1} it suffices to have $f(\tilde{z}_n) \in \frac{1}{2}U_{n+1}$. We do this by composing the Möbius transformation σ that sent 0 to $\frac{1}{2}$ in the definition of g with another Möbius transformation σ_n that sends $\frac{1}{2}$ to w_{n+1} (the center of U_{n+1}). Thus g now has a critical point in $\widetilde{D}_n$ that has critical value w_n, as desired. The points $\frac{1}{2}$ and w_{n+1} are only $O(r_{n+1})$ apart, so the new complex dilatation that is introduced into g is bounded by $O(r_{n+1})$ and is supported on an annulus of width $O(d_{p_n}^{-1})$ along the boundary of $\partial\widetilde{D}_n$. The corresponding correction we have to make to ϕ is very close to the identity on the whole plane, but we only need for it to be close to the identity on unit disks centered along the finite set $\{x_0, ..., x_{n+1}\}$, say moving points by less than $\frac{1}{1000} \cdot 2^{-n}$ in each of these disks. This follows by taking d_{p_n} large enough, and this is the second condition determining our choice of the sequence $\{d_k\}_{k=1}^{\infty}$. (There is no possible circularity here because we are simply using an estimate that says that if a K-quasiconformal map has dilatation supported in a set of area ε then the map is within $\delta(K, \varepsilon, E)$ of the identity on the compact set E.)

These errors have been chosen to be summable over n, so making the desired replacements in every $\widetilde{D}_n$ gives a new entire function F so that the nth iterate of the disk U_n under F still lands inside $\widetilde{D}_n$ and the $(n+1)$-st iterate of U_n lands inside U_{n+1}. Thus choosing any of the disks U_n satisfies the conditions of the lemma and proves that F has a wandering domain. By construction, the only critical values of F are ± 1, $\pm\frac{1}{2}$ or are part of a sequence accumulating at $\pm\frac{1}{2}$, so the singular set is bounded, i.e., $f \in \mathcal{B}$. □

Various modifications of this construction are possible. For example, by choosing U_n to iterate into itself, we can create an attracting periodic cycle that approximates the orbit of $\frac{1}{2}$ for as many steps as we wish. This gives a sequence of attracting orbits that limits on an escaping orbit.

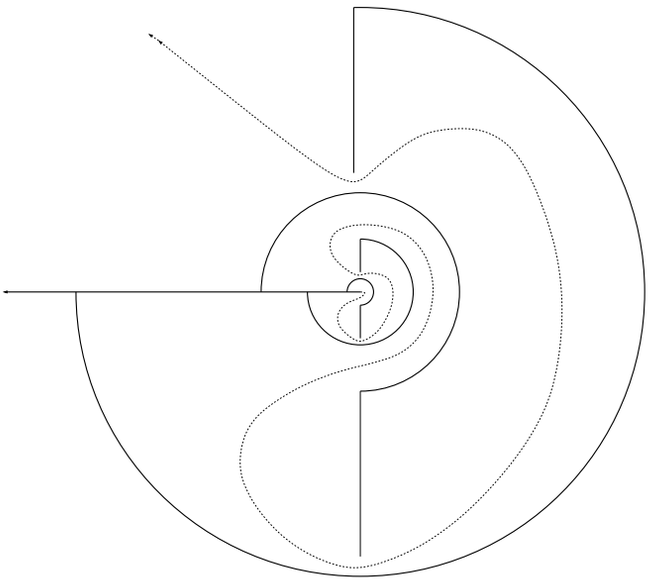

Figure 42. This is the tree for the counterexample to the strong Eremenko conjecture in $\mathcal{S}$. The tract is denoted $\Omega = \mathbb{C} \setminus T$. The dashed line shows a geodesic to ∞. Because of the change of scales, it is easier to understand this tract in cosh-coordinates. See Figure 43.

18. Application: the strong Eremenko conjecture fails in $\mathcal{S}$

The *escaping set* of f is defined as

$$I(f) = \{z : f^k(z) \to \infty \text{ as } k \to \infty\}.$$

For functions in $\mathcal{B}$, Eremenko and Lyubich [22] proved that the Julia set of f is the closure of $I(f)$. Fatou had observed that in special cases (e.g., $z \mapsto r\sin(z)$) this set contains curves tending to ∞, and in [19] Eremenko asked if every point of $I(f)$ can be connected to ∞ by a curve in $I(f)$ (the strong Eremenko conjecture). In that paper Eremenko also proved the crucial fact that the escaping set is always non-empty and placed the study of $I(f)$ at the center of transcendental dynamics.

The most striking recent results are due to Rottenfusser, Rückert, Rempe-Gillen and Schleicher in [41]. They show that the strong Eremenko conjecture is true for the class of finite-order entire functions in $\mathcal{B}$, but an infinite-order counterexample exists in $\mathcal{B}$. The techniques of this paper show that their example can be replicated in $\mathcal{S}$. We briefly sketch the argument, but refer to [41] for the details. The tree T we use is illustrated in Figure 42. Let $\Omega = \mathbb{C} \setminus T$. Because of changes in scale, it is easier to understand the example in cosh-coordinates $\Omega' = \operatorname{arcosh}(\Omega)$, as in Figure 43.

Here we see that Ω' is a horizontal half-strip that has arcs removed that force any curve in Ω' that goes to infinity to "double back" infinitely often. More precisely, we

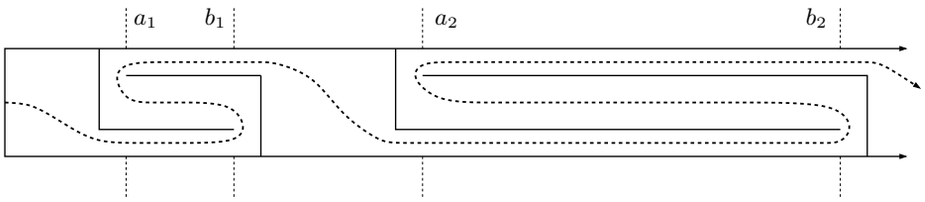

Figure 43. The domain Ω' shown here is a one-to-one conformal image of Ω in Figure 42 via the map $\cosh(\Omega')=\Omega$. Changing coordinates makes the geometry easier to understand. Any curve in Ω' that connects the left side to ∞ must cross between the lines $\{x+iy{:}x=a_n\}$ and $\{x+iy{:}x=b_n\}$ three times.

have points $a_1<b_1<a_2<\dots$, so that any such curve must cross the lines $\{x=a_1\}$, $\{x=b_1\}$, $\{x=a_1\}$ and $\{x=b_1\}$ in that order. We choose (a_n, b_n) inductively as follows. Suppose γ is any arc connecting the left side Ω' to ∞, such that $F(\gamma)\subset\Omega'$. Then the subarc of γ between the first crossing of $\{x=a_{n-1}\}$ and the last crossing of $\{x=b_{n-1}\}$ has an image under F that is contained between $\{x=a_n\}$ and $\{x=b_n\}$. This means that any arc in Ω' that connects $\{x=a_n\}$ and $\{x=b_n\}$ has an F-preimage that crosses between $\{x=a_{n-1}\}$ and $\{x=b_{n-1}\}$ at least three times.

The methods of this paper produce a quasiregular function g such that $g^{-1}([-1,1])=T$ and an entire function f that approximates g as closely as we wish; in particular $f^{-1}([-1,1])$ is as close to T as we wish. We choose $F\colon\Omega'\to\mathbb{H}_r$ so that $f=\cosh\circ F\circ\operatorname{arcosh}$ on Ω. Then iterating f is essentially the same as iterating F. The comments above apply equally well to the original T or its approximation.

Rottenfusser, Rückert, Rempe-Gillen and Schleicher now argue as follows. If there was a curve in the escaping set of f tending to ∞, then there must be a curve tending to ∞ in Ω' that maps to itself under F. Since it crosses at least once between $\{x=a_n\}$ and $\{x=b_n\}$, it crosses between $\{x=a_{n-1}\}$ and $\{x=b_{n-1}\}$ at least three times. Proceeding by induction, the curve crosses between $\{x=a_1\}$ and $\{x=b_1\}$ at least 3^{n-1} times. As n was arbitrary, this is impossible, so the escaping set contains no curve going to ∞. Since $b_n/a_n\to\infty$, it is easy to see that our example has infinite order, and indeed, another result in [41] says that the strong Eremenko conjecture holds for finite-order elements of $\mathcal{B}$.

Rottenfusser, Rückert, Rempe-Gillen and Schleicher also showed that there is an element of $\mathcal{B}$ whose Julia set has no non-trivial path-connected components, and this example can also be constructed in $\mathcal{S}$. Note that, as above, no new dynamical argument is needed; we simply apply our $\mathcal{S}$ approximation results to the dynamical model constructed in [41].

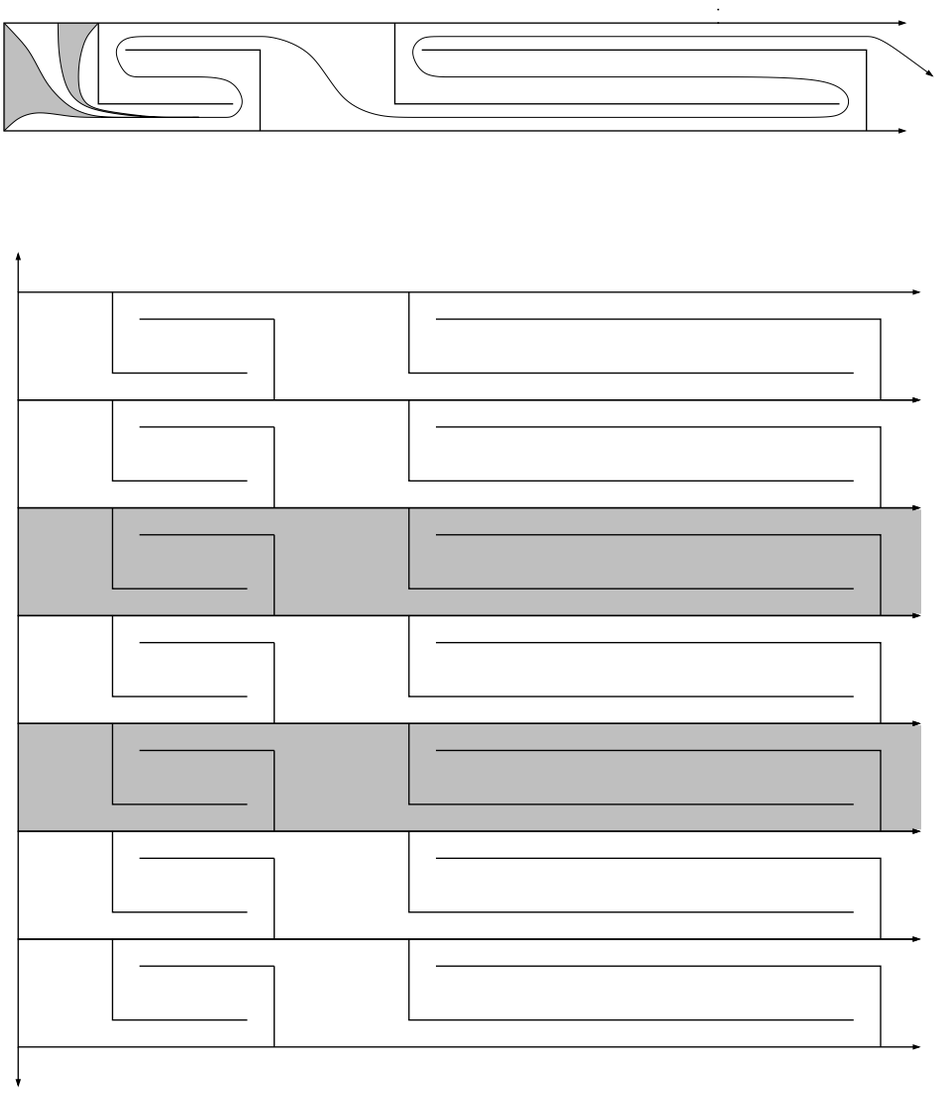

Figure 44. The conformal map F maps each copy of Ω' conformally to the half-plane. Thus each copy of Ω' contains countable many preimages of copies of itself. On the bottom, two copies are shaded and possible preimages of these two copies are shown in the top (this is a sketch, not a computation). Each preimage connects $\{x{=}a_1\}$ and $\{x{=}b_1\}$ three times. The preimages of these preimages connect these lines nine times. In the limit, the two lines are connected arbitrarily often by a connected component of the escaping set, and hence these components are not curves.

References

[1] Baker, I. N., Multiply connected domains of normality in iteration theory. *Math. Z.*, 81 (1963), 206–214.

[2] — The domains of normality of an entire function. *Ann. Acad. Sci. Fenn. Ser. A I Math.*, 1 (1975), 277–283.

[3] — An entire function which has wandering domains. *J. Austral. Math. Soc. Ser. A*, 22 (1976), 173–176.

[4] Belyĭ, G. V., Galois extensions of a maximal cyclotomic field. *Izv. Akad. Nauk SSSR Ser. Mat.*, 43 (1979), 267–276, 479 (Russian); English translation in *Math. USSR–Izv.*, 14 (1980), 247–256.

[5] Bergweiler, W., Iteration of meromorphic functions. *Bull. Amer. Math. Soc.*, 29 (1993), 151–188.

[6] Bergweiler, W. & Eremenko, A., Entire functions of slow growth whose Julia set coincides with the plane. *Ergodic Theory Dynam. Systems*, 20 (2000), 1577–1582.

[7] Bergweiler, W., Haruta, M., Kriete, H., Meier, H.-G. & Terglane, N., On the limit functions of iterates in wandering domains. *Ann. Acad. Sci. Fenn. Ser. A I Math.*, 18 (1993), 369–375.

[8] Beurling, A., Some theorems on boundedness of analytic functions. *Duke Math. J.*, 16 (1949), 355–359.

[9] Bishop, C. J., A transcendental Julia set of dimension 1. Preprint, 2011.

[10] — True trees are dense. *Invent. Math.*, 197 (2014), 433–452.

[11] — Models for the Eremenko–Lyubich class. Preprint, 2014.

[12] — Models for the Speiser class. Preprint, 2014.

[13] — The order conjecture fails in class S. To appear in *J. Anal. Math.*

[14] Branner, B. & Fagella, N., *Quasiconformal Surgery in Holomorphic Dynamics*. Cambridge Studies in Advanced Mathematics, 141. Cambridge University Press, Cambridge, 2014.

[15] Cámera, G. A., On a problem of Erdős. *Acta Cient. Venezolana*, 34 (1983), 191–194.

[16] Drasin, D., Gol′dberg, A. A. & Poggi-Corradini, P., Quasiconformal mappings in value-distribution theory, in *Handbook of Complex Analysis*: *Geometric Function Theory*. Vol. 2, pp. 755–808. Elsevier, Amsterdam, 2005.

[17] Dyn′kin, E. M., Smoothness of a quasiconformal mapping at a point. *Algebra i Analiz*, 9 (1997), 205–210 (Russian); English translation in *St. Petersburg Math. J.*, 9 (1998), 601–605.

[18] Epstein, A., *Towers of Finite Type Complex Analytic Maps*. Ph.D. Thesis, City University of New York, New York, NY, 1995. http://pcwww.liv.ac.uk/~lrempe/adam/thesis.pdf.

[19] Eremenko, A., On the iteration of entire functions, in *Dynamical Systems and Ergodic Theory* (Warsaw, 1986), Banach Center Publ., 23, pp. 339–345. PWN – Polish Scientific Publishers, Warsaw, 1989.

[20] — Transcendental meromorphic functions with three singular values. *Illinois J. Math.*, 48 (2004), 701–709.

[21] Eremenko, A. & Lyubich, M. Yu., Examples of entire functions with pathological dynamics. *J. London Math. Soc.*, 36 (1987), 458–468.

[22] — Dynamical properties of some classes of entire functions. *Ann. Inst. Fourier* (*Grenoble*), 42 (1992), 989–1020.

[23] Fagella, N., Godillion, S. & Jarque, X., Wandering domains for composition of entire functions. Preprint, 2014. arXiv:1410.3221 [math.DS].

[24] GARNETT, J. B. & MARSHALL, D., *Harmonic Measure*. New Mathematical Monographs, 2. Cambridge University Press, Cambridge, 2005.

[25] GAUTHIER, P., Unbounded holomorphic functions bounded on a spiral. *Math. Z.*, 114 (1970), 278–280.

[26] GOL′DBERG, A. A., Sets on which the modulus of an entire function has a lower bound. *Sibirsk. Mat. Zh.*, 20 (1979), 512–518, 691 (Russian); English translation in *Siberian Math. J.*, 20 (1979), 360–364.

[27] GOL′DBERG, A. A. & OSTROVSKII, I. V., *Value Distribution of Meromorphic Functions*. Translations of Mathematical Monographs, 236. Amer. Math. Soc., Providence, RI, 2008.

[28] GOLDBERG, L. & KEEN, L., A finiteness theorem for a dynamical class of entire functions. *Ergodic Theory Dynam. Systems*, 6 (1986), 183–192.

[29] HAYMAN, W. K., The minimum modulus of large integral functions. *Proc. London Math. Soc.*, 2 (1952), 469–512.

[30] — Research problems in function theory: new problems, in *Proceedings of the Symposium on Complex Analysis* (Canterbury, 1973), London Math. Soc. Lecture Note Ser., 12, pp. 155–180. Cambridge Univ. Press, London, 1974.

[31] HE, Z.-X. & SCHRAMM, O., Fixed points, Koebe uniformization and circle packings. *Ann. of Math.*, 137 (1993), 369–406.

[32] HEINS, M., The set of asymptotic values of an entire function, in *Tolfte Skandinaviska Matematikerkongressen* (Lund, 1953), pp. 56–60. Lunds Universitets Matematiska Institution, Lund, 1954.

[33] HINCHLIFFE, J. D., The Bergweiler–Eremenko theorem for finite lower order. *Results Math.*, 43 (2003), 121–128.

[34] KOCHETKOV, YU. YU., On the geometry of a class of plane trees. *Funktsional. Anal. i Prilozhen.*, 33 (1999), 78–81 (Russian); English translation in *Funct. Anal. Appl.*, 33 (1999), 304–306.

[35] — Geometry of planar trees. *Fundam. Prikl. Mat.*, 13 (2007), 149–158 (Russian); English translation in *J. Math. Sci. (N.Y.)*, 158 (2009), 106–113.

[36] LANGLEY, J. K., On differential polynomials, fixpoints and critical values of meromorphic functions. *Results Math.*, 35 (1999), 284–309.

[37] MERENKOV, S., Rapidly growing entire functions with three singular values. *Illinois J. Math.*, 52 (2008), 473–491.

[38] MIHALJEVIĆ-BRANDT, H. & REMPE-GILLEN, L., Absence of wandering domains for some real entire functions with bounded singular sets. *Math. Ann.*, 357 (2013), 1577–1604.

[39] REMPE-GILLEN, L., Hyperbolic entire functions with full hyperbolic dimension and approximation by Eremenko–Lyubich functions. *Proc. Lond. Math. Soc.*, 108 (2014), 1193–1225.

[40] REMPE-GILLEN, L. & RIPPON, P., Exotic Baker and wandering domains for Ahlfors islands maps. *J. Anal. Math.*, 117 (2012), 297–319.

[41] ROTTENFUSSER, G., RÜCKERT, J., REMPE-GILLEN, L. & SCHLEICHER, D., Dynamic rays of bounded-type entire functions. *Ann. of Math.*, 173 (2011), 77–125.

[42] SCHLEICHER, D., Dynamics of entire functions, in *Holomorphic Dynamical Systems*, Lecture Notes in Math., 1998, pp. 295–339. Springer, Berlin, 2010.

[43] SHABAT, G. & ZVONKIN, A., Plane trees and algebraic numbers, in *Jerusalem Combinatorics '93*, Contemp. Math., 178, pp. 233–275. Amer. Math. Soc., Providence, RI, 1994.

[44] STALLARD, G., The Hausdorff dimension of Julia sets of entire functions. II. *Math. Proc. Cambridge Philos. Soc.*, 119 (1996), 513–536.

[45] — The Hausdorff dimension of Julia sets of entire functions. III. *Math. Proc. Cambridge Philos. Soc.*, 122 (1997), 223–244.

[46] Sullivan, D., Quasiconformal homeomorphisms and dynamics. I. Solution of the Fatou–Julia problem on wandering domains. *Ann. of Math.*, 122 (1985), 401–418.

[47] Teichmüller, O., Eine Umkehrung des zweiten Hauptsatzes der Wertverteilungslehre. *Deutsche Math.*, 2 (1937), 96–107.

[48] Wiman, A., Über den Zusammenhang zwischen dem Maximalbetrage einer analytischen Funktion und dem grössten Betrage bei gegebenem Argumente der Funktion. *Acta Math.*, 41 (1916), 1–28.

[49] Wittich, H., Zum Beweis eines Satzes über quasikonforme Abbildungen. *Math. Z.*, 51 (1948), 278–288.

Christopher J. Bishop
Mathematics Department
Stony Brook University
Stony Brook, NY 11794-3651
U.S.A.
bishop@math.sunysb.edu

Received May 10, 2013
Received in revised form August 12, 2014